Electronic Supplementary Information

Hydrogenation Reactions Catalyzed by $HN(CH_2CH_2PR_2)_2$-Ligated Copper Complexes

*Dewmi A. Ekanayake, Arundhoti Chakraborty, Jeanette A. Krause, and Hairong Guan**

Department of Chemistry, University of Cincinnati, P.O. Box 210172, Cincinnati, Ohio 45221-0172, United States

*E-Mail: hairong.guan@uc.edu

Table of Contents

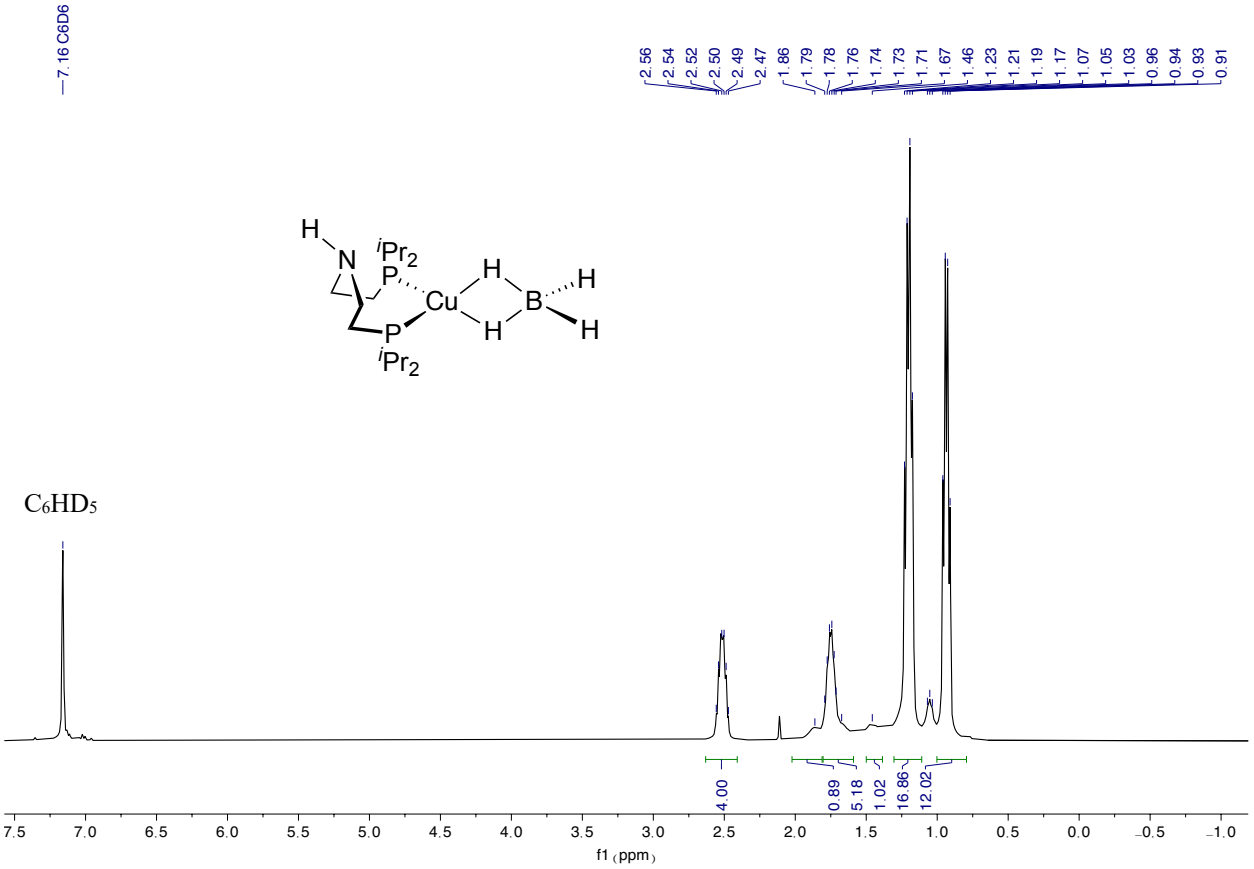

Figure S1. ^{1}H NMR (400 MHz, C_6D_6, 23 °C) spectrum of ($^{i\text{Pr}}$PN$^{\text{H}}$P)Cu(BH_4) (**2a**): 2.63-2.41 (m, NCH_2, 4H), 1.83-1.69 (m, PCH(CH_3)$_2$, 4H), likely 1.56 (q, $J_{\text{H-B}}$ = 82 Hz, BH_4, 4H), 1.26-1.13 (m, CH(CH_3)$_2$ + PCH_2, 16H), 1.00-0.83 (m, CH(CH_3)$_2$, 12H); the NH resonance is not located.

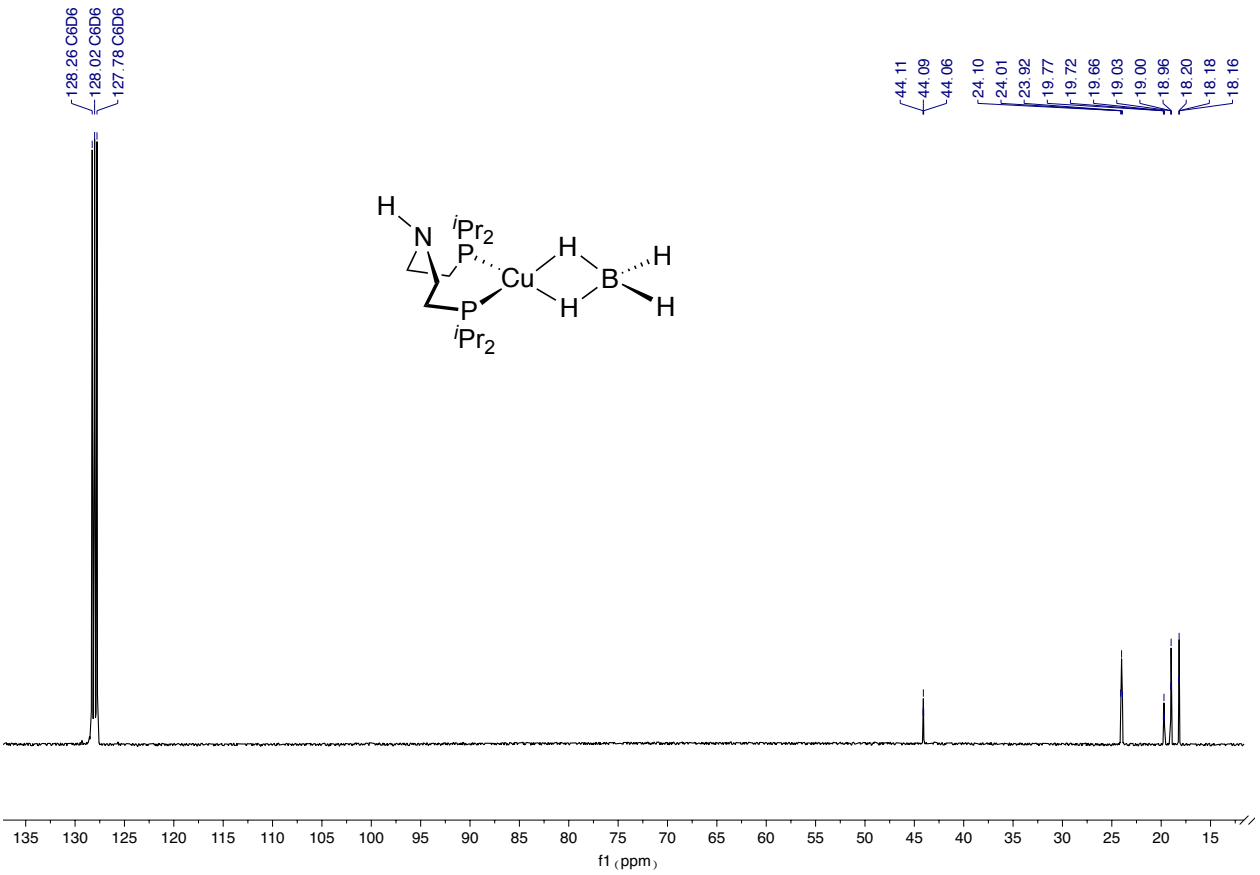

Figure S2. $^{13}C\{^{1}H\}$ NMR (101 MHz, C_6D_6, 23 °C) spectrum of ($^{i\text{Pr}}PN^{H}P$)Cu(BH_4) (**2a**): 44.1 (t, $J_{C\text{-}P}$ = 2.7 Hz, NCH_2), 24.0 (t, $J_{C\text{-}P}$ = 9.3 Hz, $CH(CH_3)_2$), 19.7 (t, $J_{C\text{-}P}$ = 5.7 Hz, PCH_2), 19.0 (t, $J_{C\text{-}P}$ = 3.5 Hz, CH(CH_3)$_2$), 18.2 (t, $J_{C\text{-}P}$ = 2.2 Hz, CH(CH_3)$_2$).

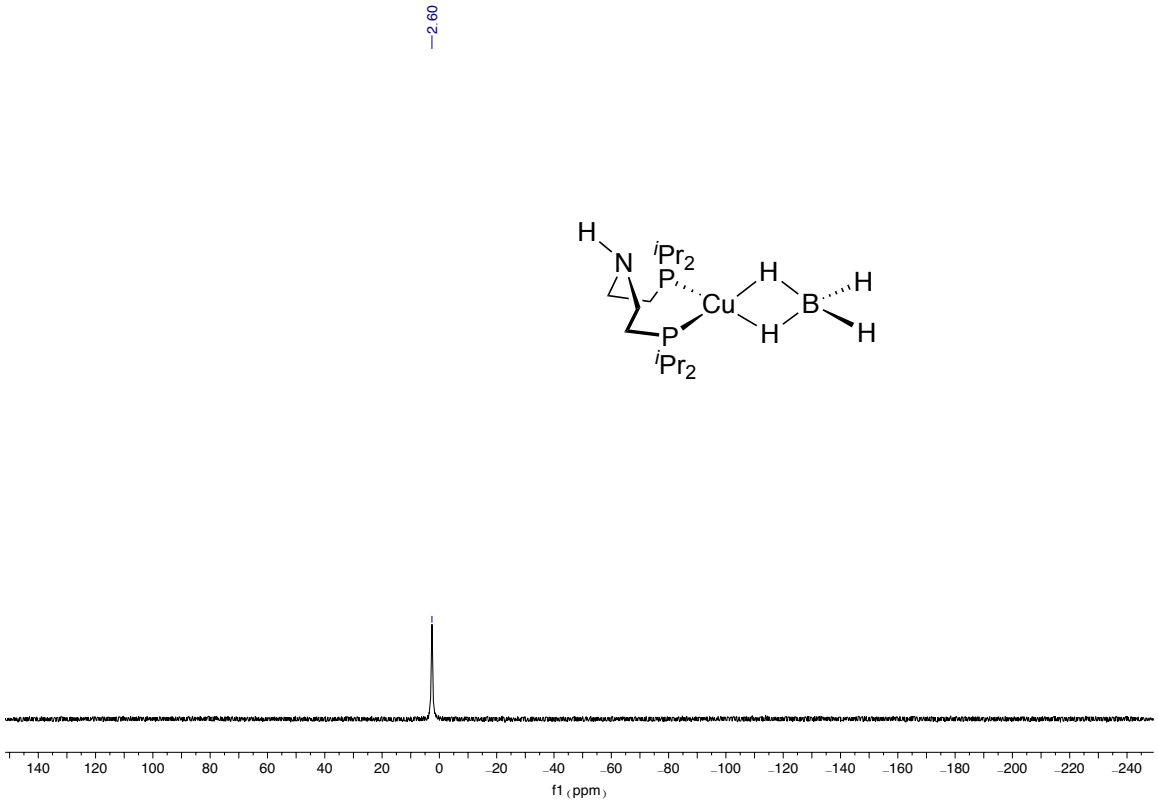

Figure S3. $^{31}P\{^{1}H\}$ NMR (162 MHz, C_6D_6, 23 °C) spectrum of ($^{i\text{Pr}}PN^{H}P$)Cu(BH_4) (**2a**)

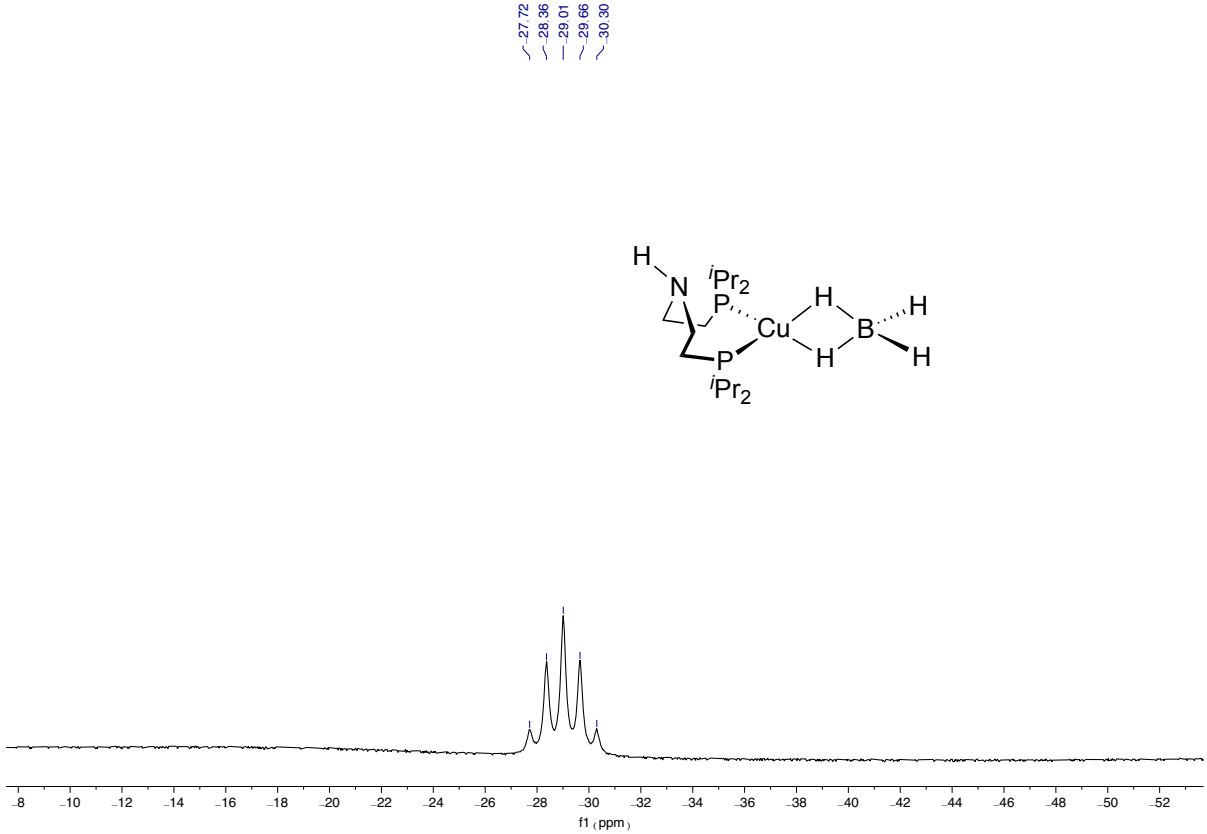

Figure S4. ^{11}B NMR (128 MHz, C_6D_6, 23 °C) spectrum of ($^{i\text{Pr}}PN^{H}P$)Cu(BH_4) (**2a**)

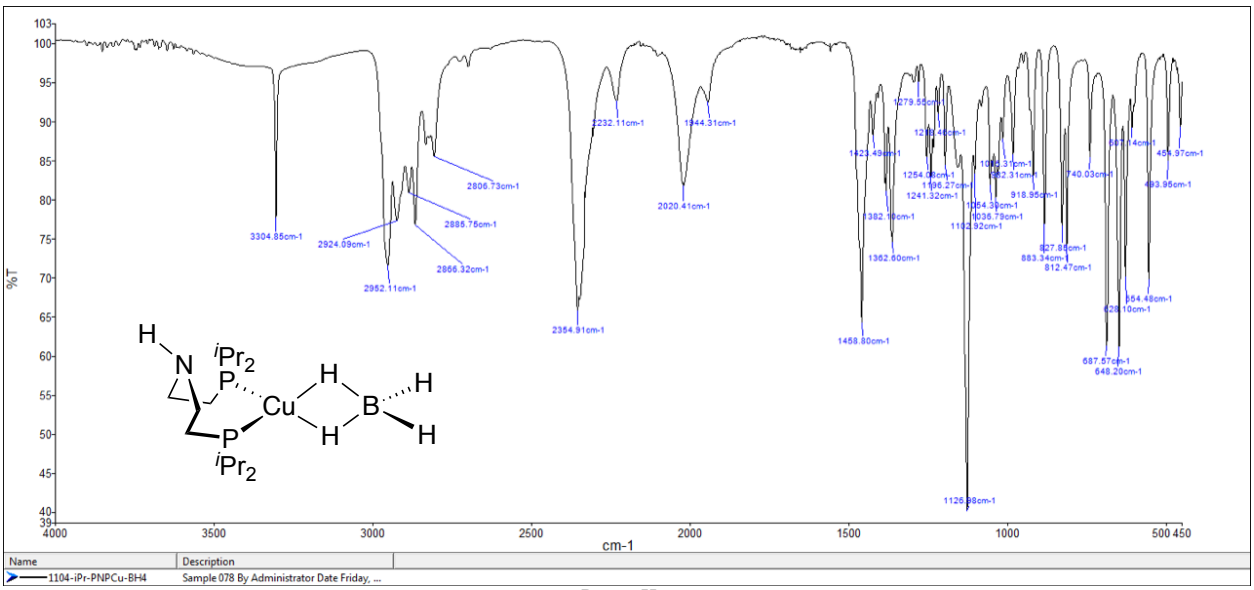

Figure S5. IR spectrum of ($^{i\mathrm{Pr}}$PN$^{\mathrm{H}}$P)Cu(BH$_4$) (**2a**, solid sample)

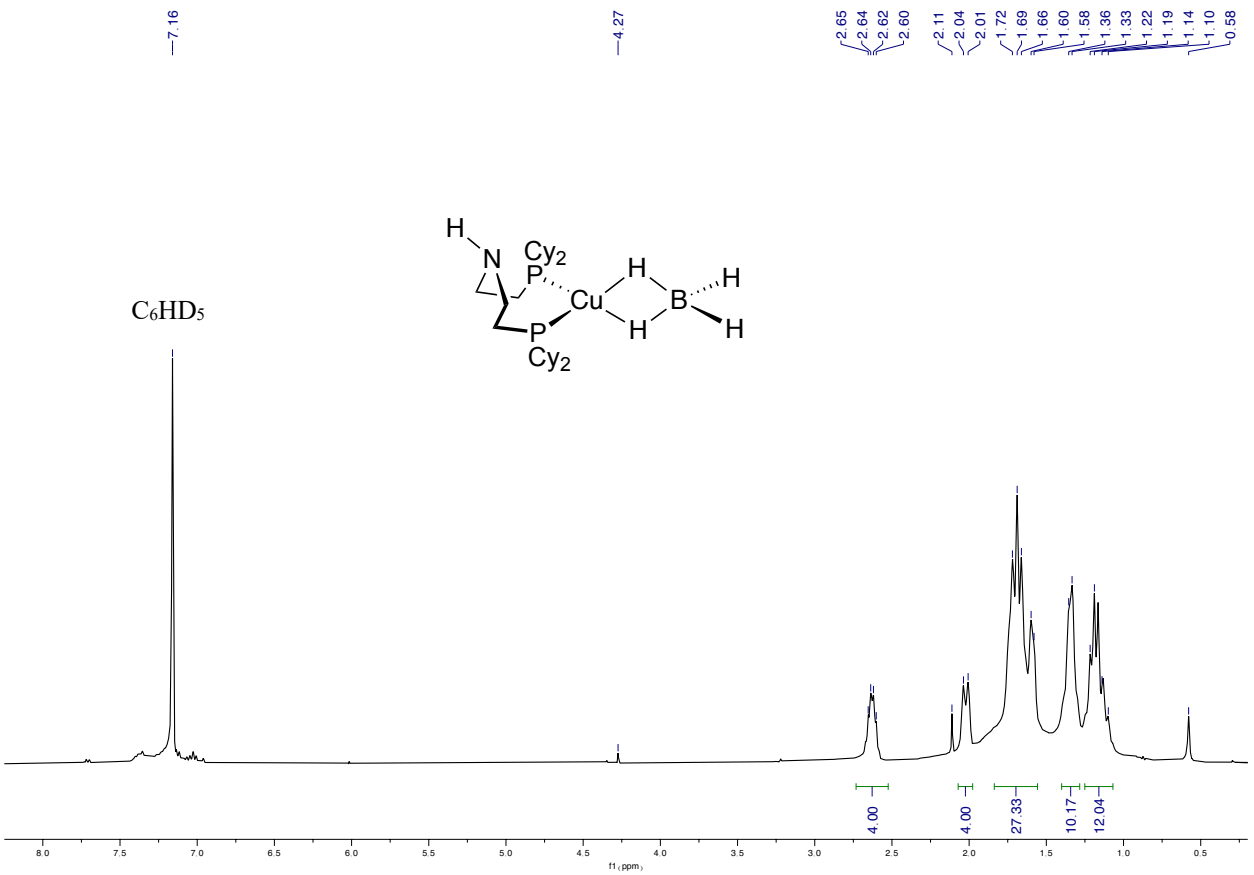

Figure S6. ^{1}H NMR (400 MHz, C_6D_6, 23 °C) spectrum of ($^{\mathrm{Cy}}$PN$^{\mathrm{H}}$P)Cu(BH$_4$) (**2b**): 2.73-2.53 (m, NC*H*$_2$, 4H), 2.08-1.97 (m, 4H), 1.84-1.56 (m, 27H), 1.40-1.28 (m, 10H), 1.25-1.07 (m, Cy*H*, 12H); the NH and BH resonances are not located.

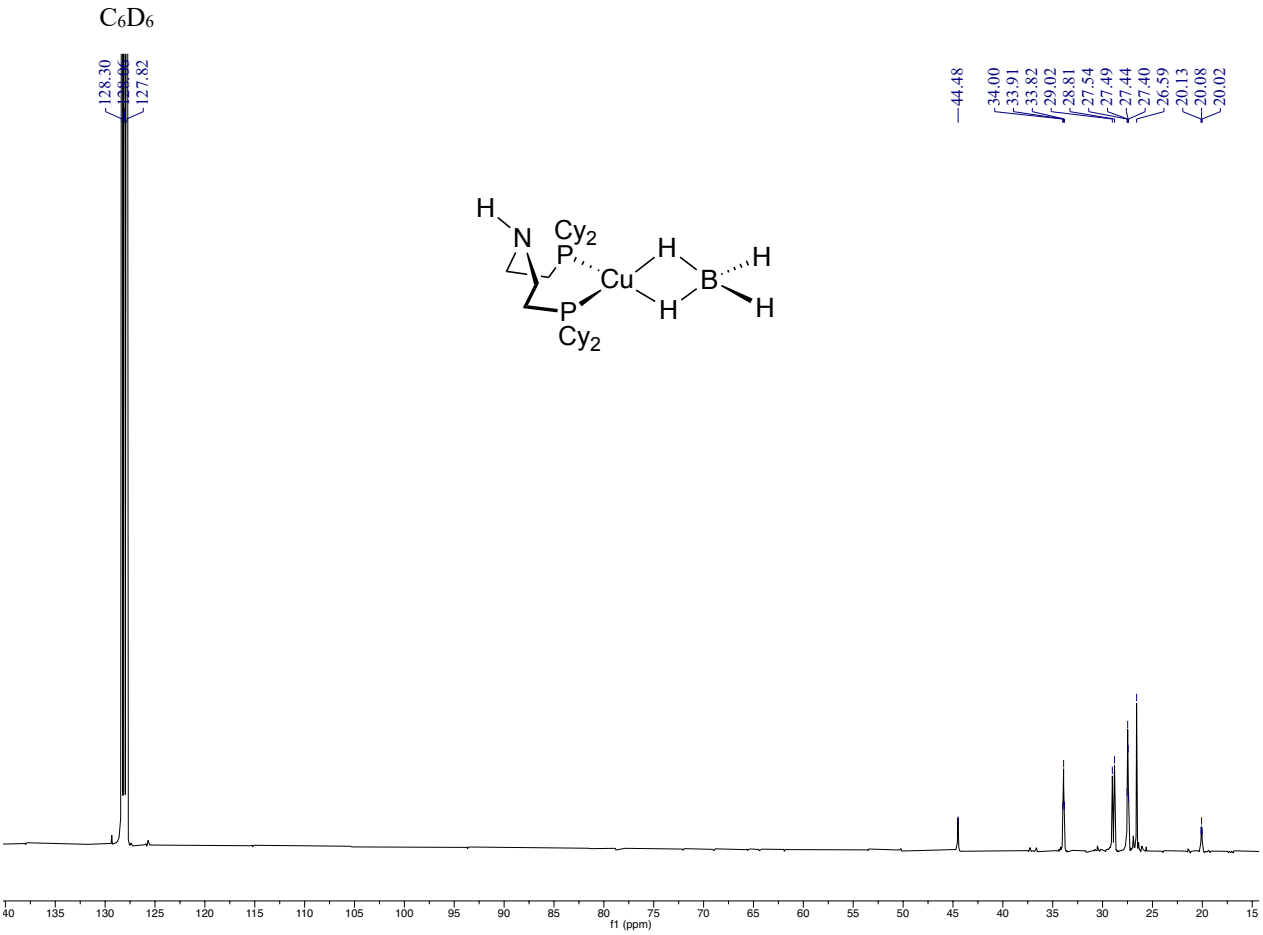

Figure S7. $^{13}C\{^{1}H\}$ NMR (101 MHz, C_6D_6, 23 °C) spectrum of ($^{Cy}PN^{H}P$)Cu(BH_4) (**2b**): 44.5 (s, N*C*H_2), 33.9 (t, $J_{C\text{-}P}$ = 8.8 Hz, P*C*H), 29.0 (s, Cy*C*), 28.8 (s, Cy*C*), 27.5 (t, $J_{C\text{-}P}$ = 5.9 Hz, Cy*C*), 27.4 (t, $J_{C\text{-}P}$ = 4.3 Hz, Cy*C*), 26.6 (s, Cy*C*), 20.1 (t, $J_{C\text{-}P}$ = 5.9 Hz, P*C*H_2).

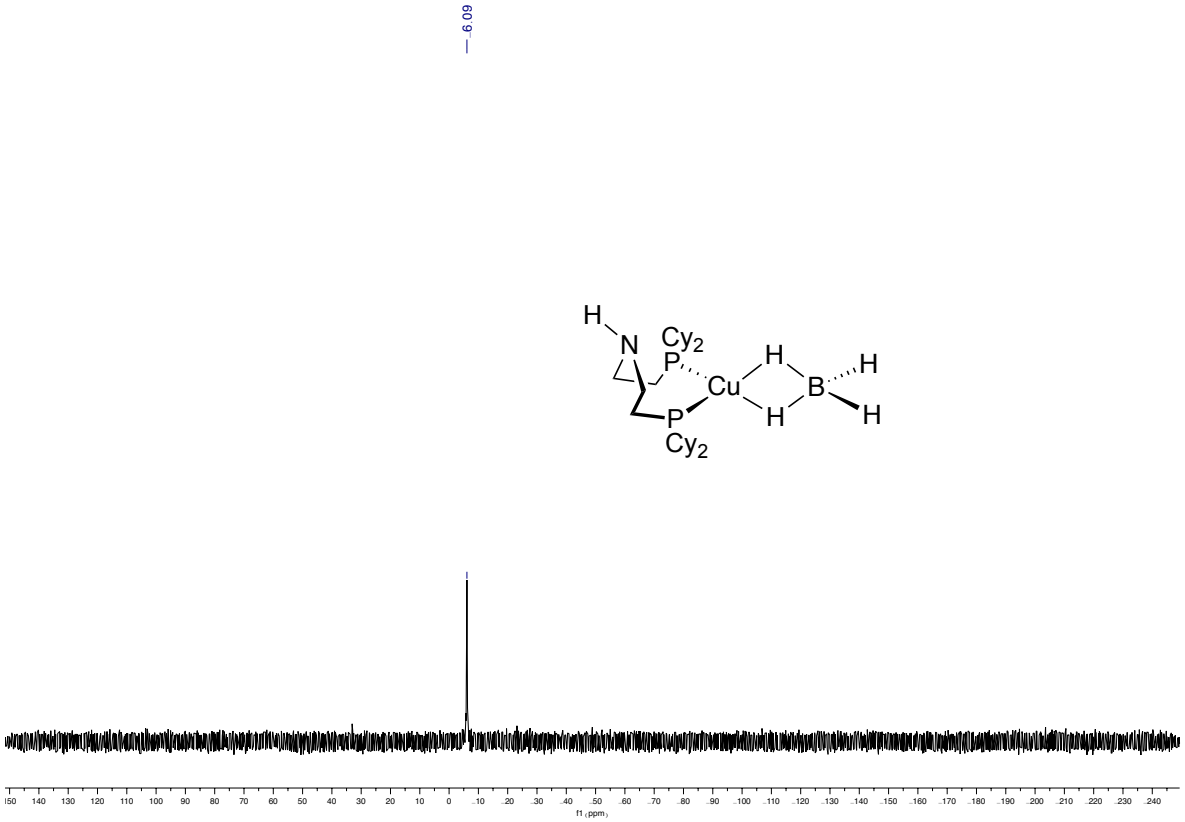

Figure S8. $^{31}P\{^{1}H\}$ NMR (162 MHz, C_6D_6, 23 °C) spectrum of ($^{Cy}PN^{H}P$)Cu(BH_4) (**2b**)

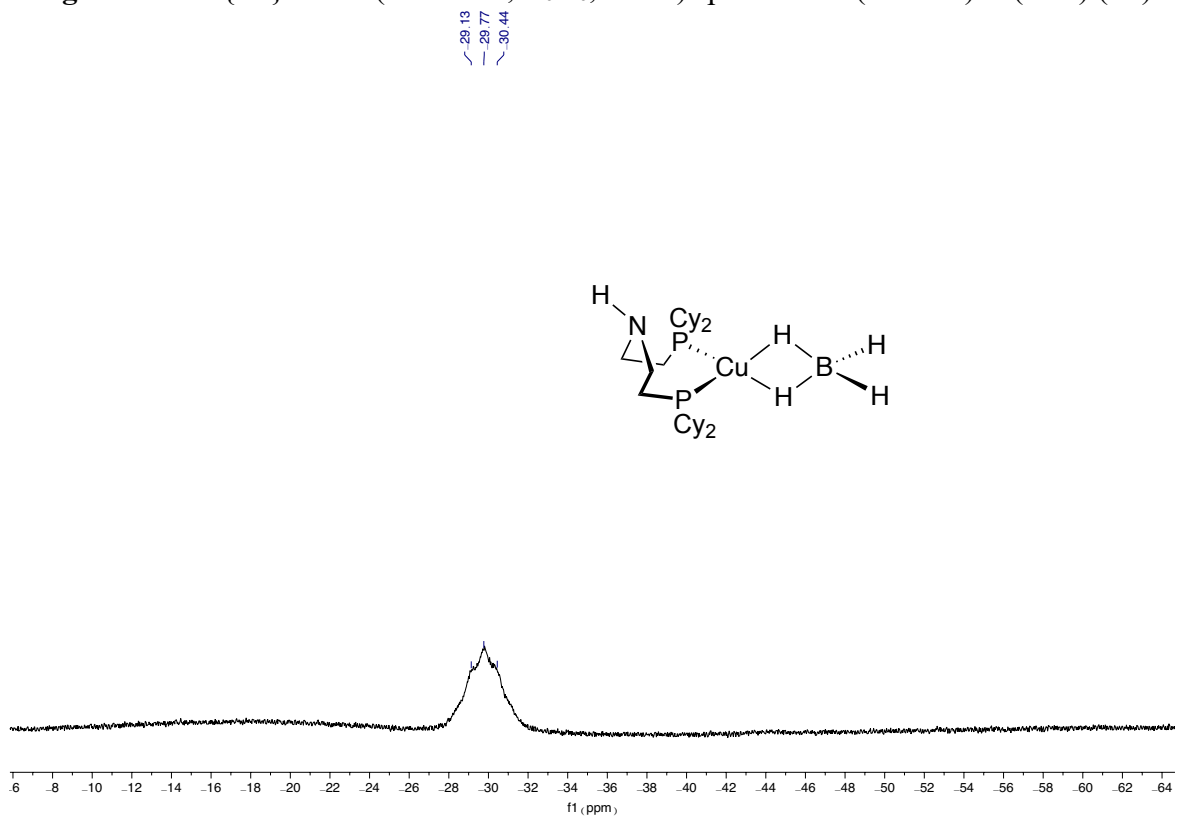

Figure S9. ^{11}B NMR (128 MHz, C_6D_6, 23 °C) spectrum of ($^{Cy}PN^{H}P$)Cu(BH_4) (**2b**)

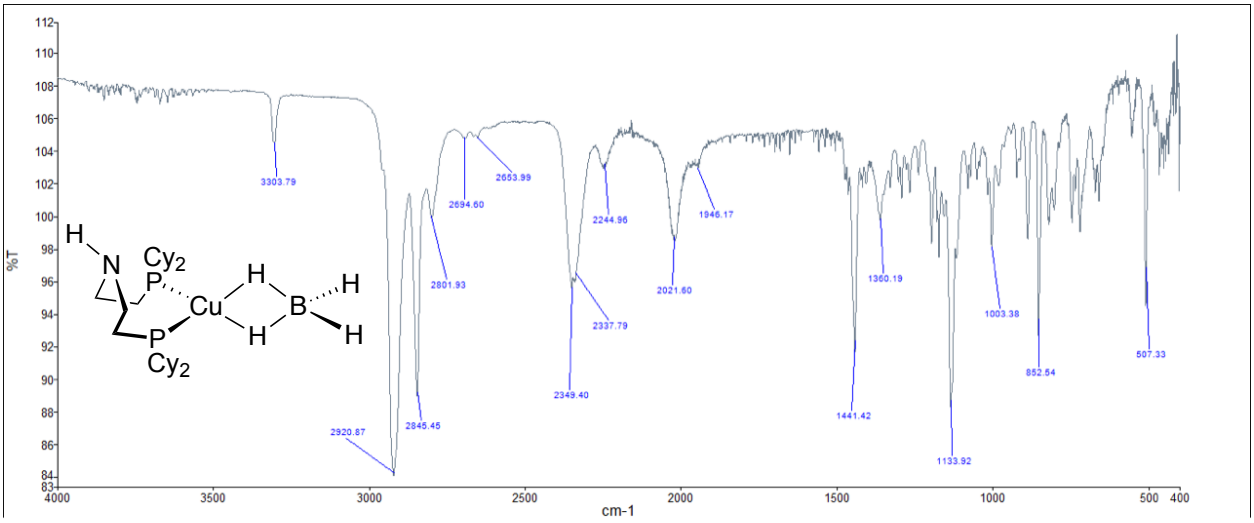

Figure S10. IR spectrum of (^{Cy}PN^{H}P)Cu(BH$_4$) (**2b**, solid sample)

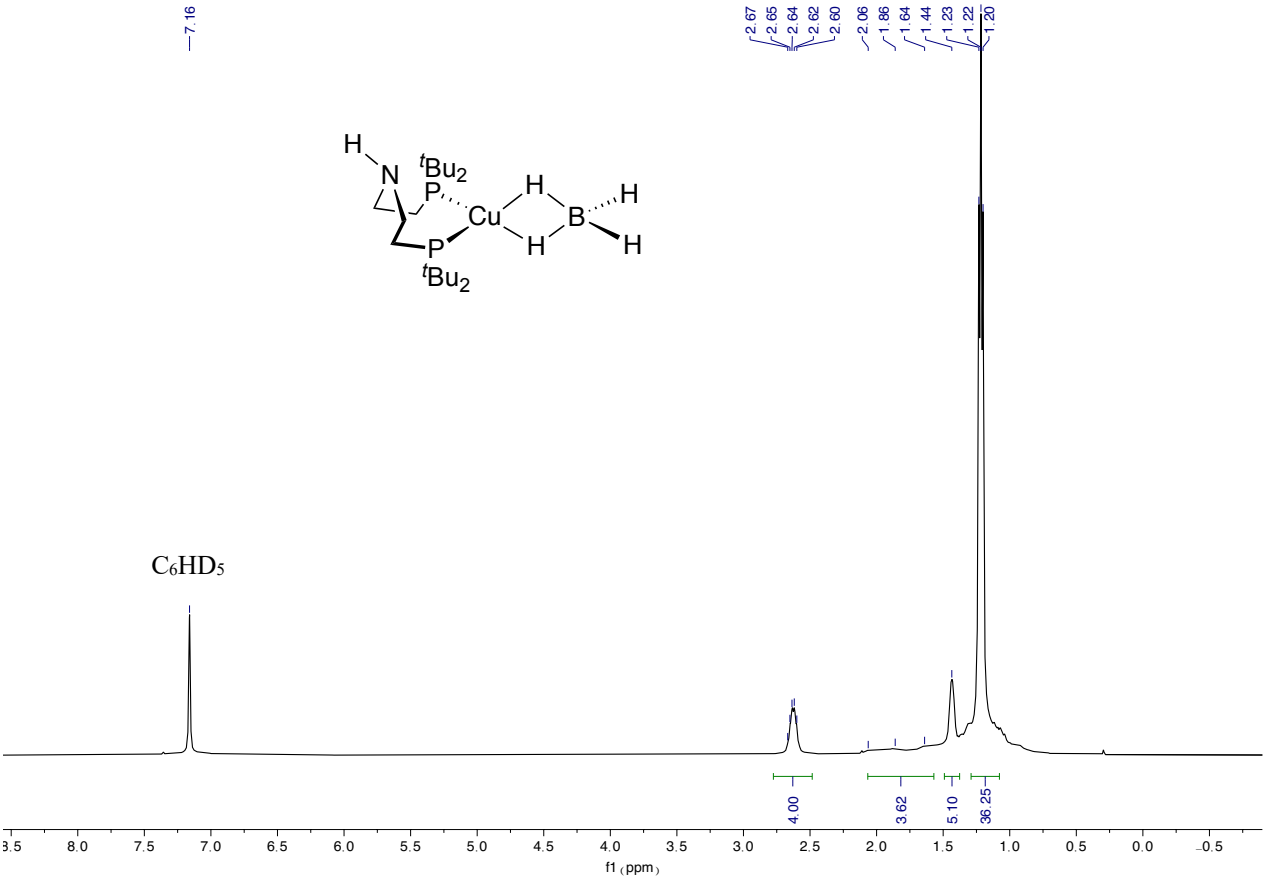

Figure S11. ^{1}H NMR (400 MHz, C_6D_6, 23 °C) spectrum of (^{tBu}PN^{H}P)Cu(BH$_4$) (**2c**): 2.70-2.56 (m, NCH_2, 4H), likely 1.75 (q, $J_{H\text{-}B}$ = 85 Hz, BH_4, 4H), 1.50-1.38 (m, PCH_2, 4H), 1.36-1.07 (m, C(CH_3)$_3$, 36H); the NH resonance is not located.

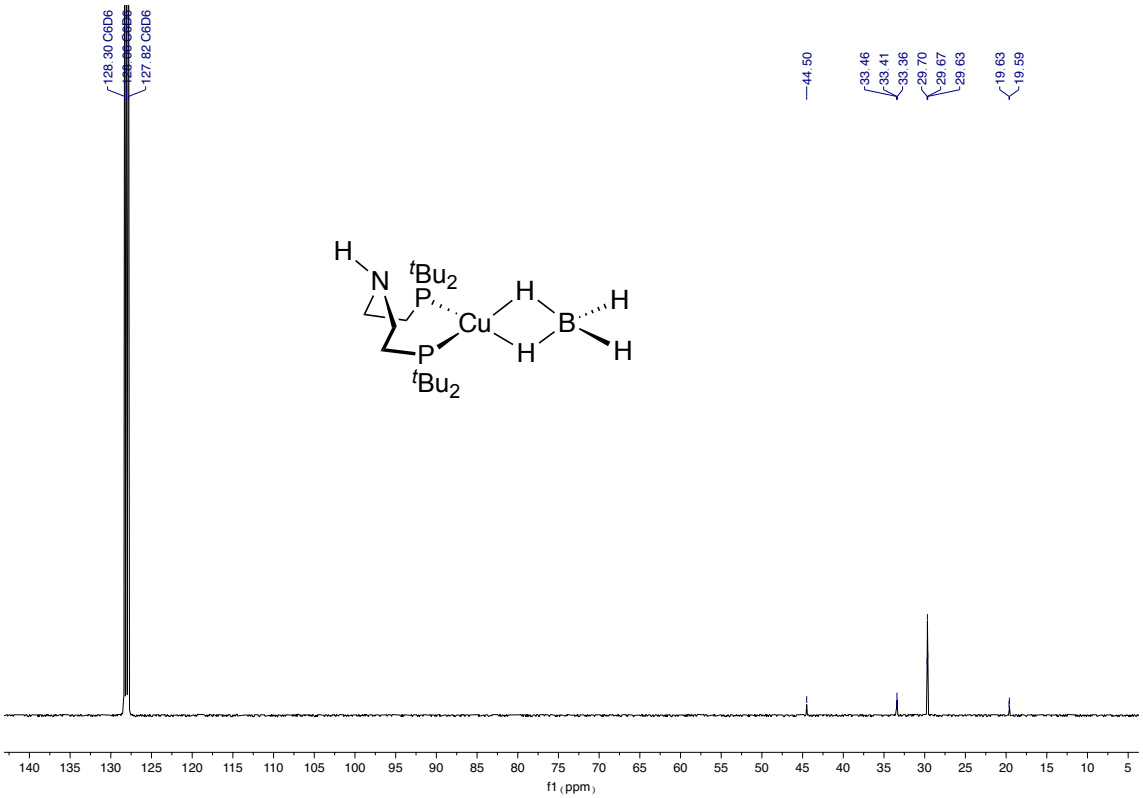

Figure S12. $^{13}C\{^{1}H\}$ NMR (101 MHz, C_6D_6, 23 °C) spectrum of ($^{t\text{Bu}}PN^{H}P$)Cu(BH_4) (**2c**): 44.5 (s, N*C*H_2), 33.4 (t, $J_{C\text{-}P}$ = 5.5 Hz, *C*(CH_3)$_3$), 29.7 (t, $J_{C\text{-}P}$ = 3.8 Hz, C(*C*H_3)$_3$), 19.6 (t, $J_{C\text{-}P}$ = 4.0 Hz, P*C*H_2).

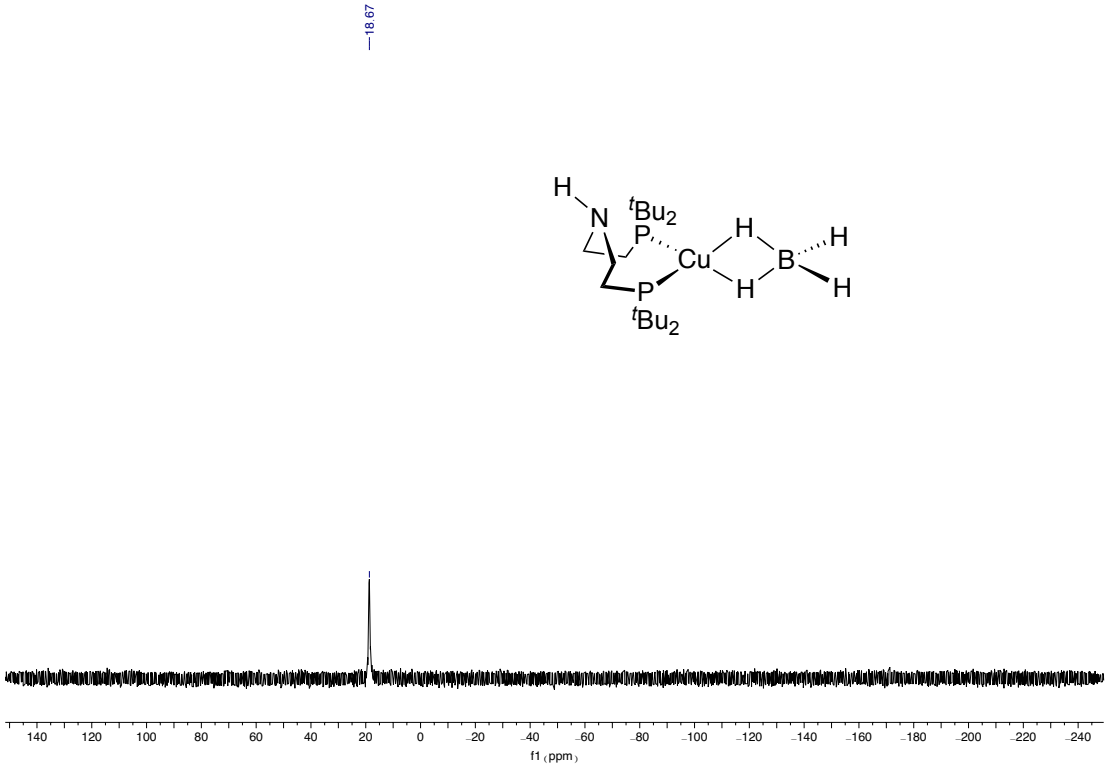

Figure S13. $^{31}P\{^{1}H\}$ NMR (162 MHz, C_6D_6, 23 °C) spectrum of ($^{t\text{Bu}}PN^{H}P$)Cu(BH_4) (**2c**)

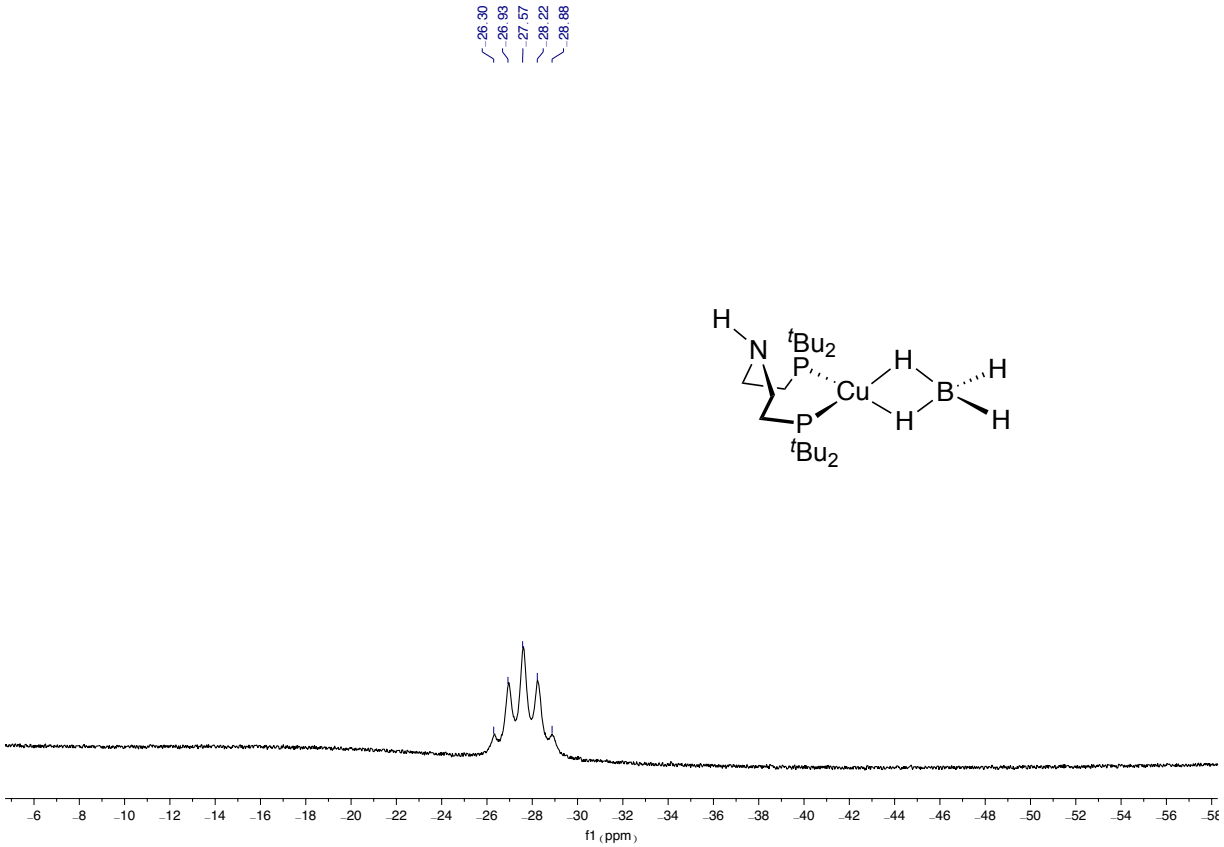

Figure S14. ^{11}B NMR (128 MHz, C_6D_6, 23 °C) spectrum of ($^{t\text{Bu}}$PN$^{\text{H}}$P)Cu(BH_4) (**2c**)

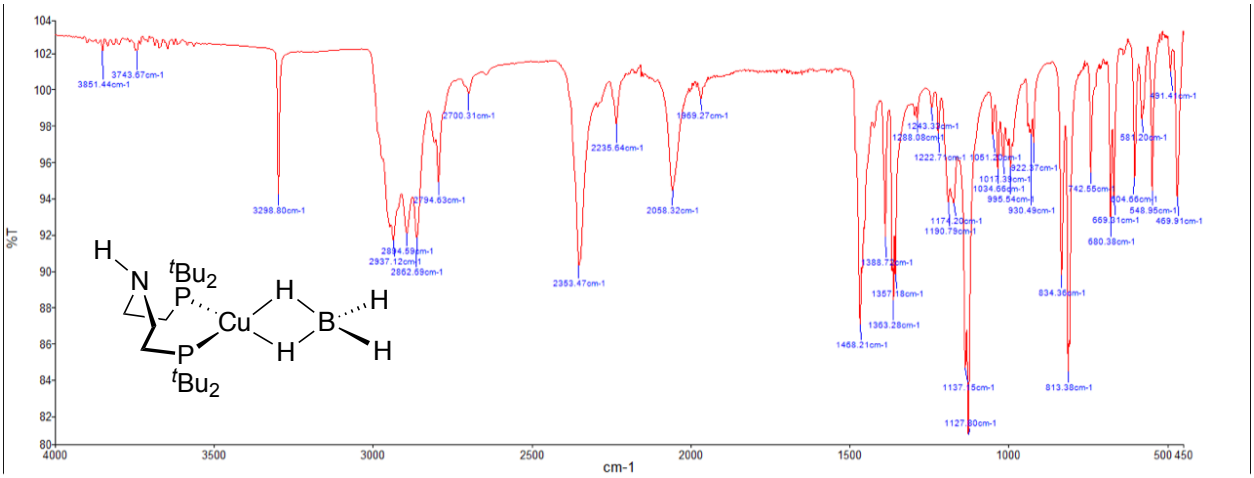

Figure S15. IR spectrum of ($^{t\text{Bu}}$PN$^{\text{H}}$P)Cu(BH_4) (**2c**, solid sample)

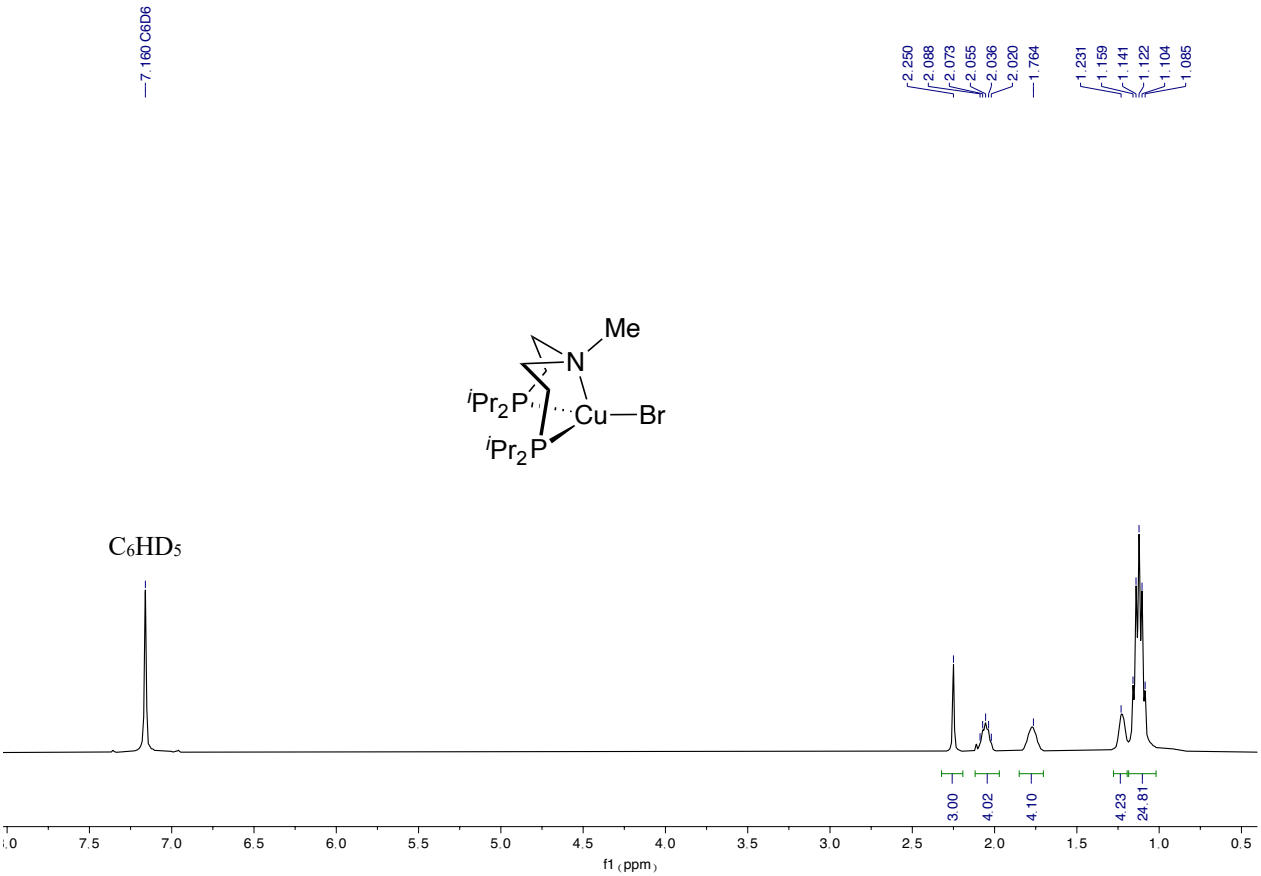

Figure S16. ^{1}H NMR (400 MHz, C_6D_6, 23 °C) spectrum of ($^{i\text{Pr}}$PN$^{\text{Me}}$P)CuBr (**4a**): 2.25 (s, NCH_3, 3H), 2.13-1.98 (m, 4H), 1.85-1.71 (m, 4H), 1.28-1.20 (m, 4H), 1.19-1.02 (m, CH(CH_3)$_2$, 24H).

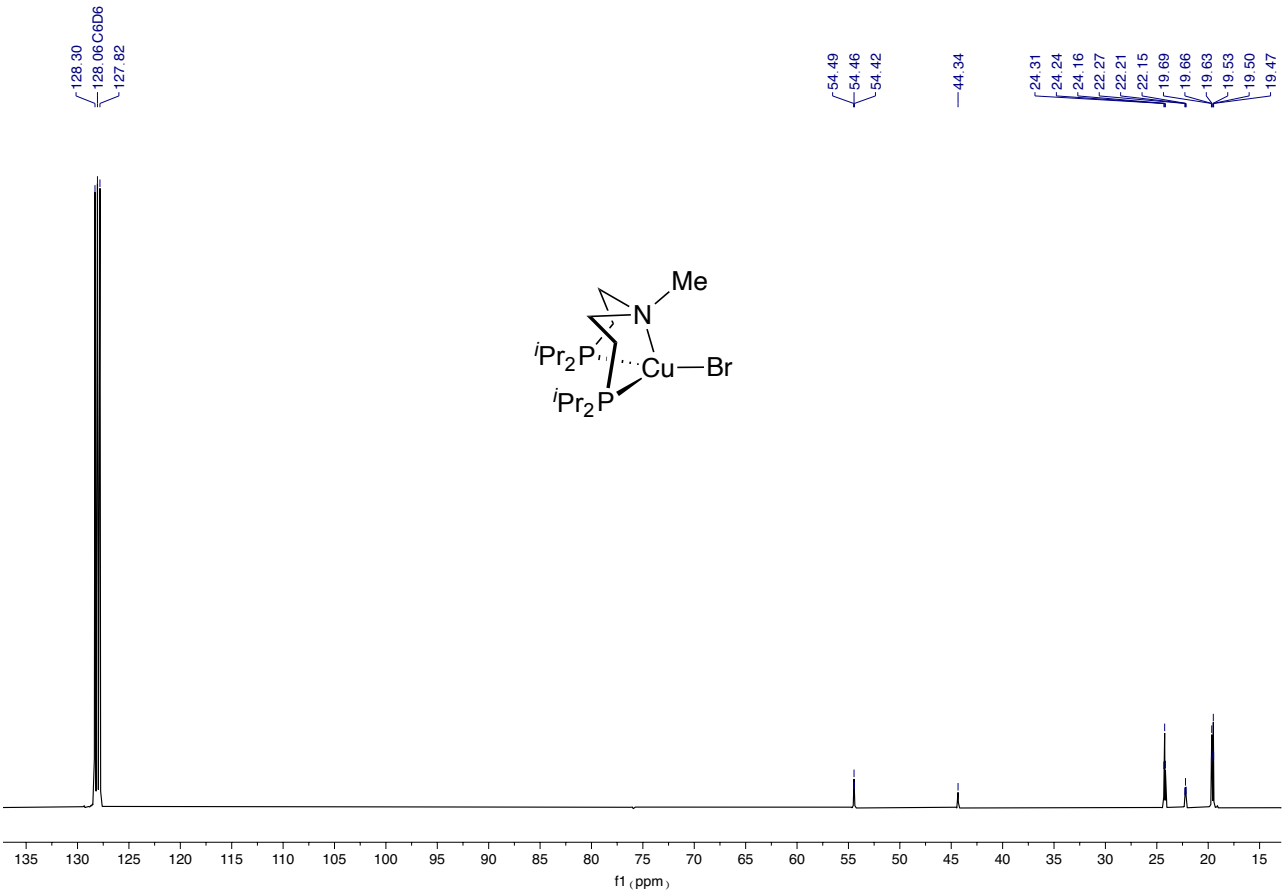

Figure S17. $^{13}C\{^{1}H\}$ NMR (101 MHz, C_6D_6, 23 °C) spectrum of ($^{i\text{Pr}}PN^{\text{Me}}P$)CuBr (**4a**): 54.5 (t, $J_{C\text{-}P}$ = 3.5 Hz, N*C*H$_3$), 44.3 (s, N*C*H$_2$), 24.2 (t, $J_{C\text{-}P}$ = 7.5 Hz, *C*H(CH$_3$)$_2$), 22.2 (t, $J_{C\text{-}P}$ = 6.4 Hz, P*C*H$_2$), 19.7 (t, $J_{C\text{-}P}$ = 2.9 Hz, CH(*C*H$_3$)$_2$), 19.5 (t, $J_{C\text{-}P}$ = 3.0 Hz, CH(*C*H$_3$)$_2$).

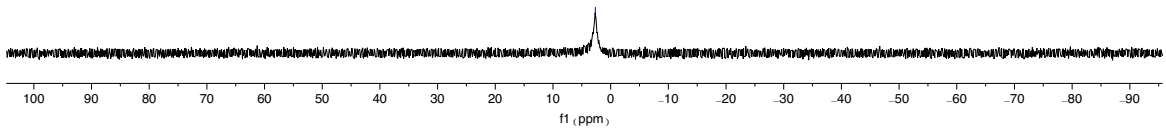

Figure S18. $^{31}P\{^{1}H\}$ NMR (162 MHz, C_6D_6, 23 °C) spectrum of ($^{i\text{Pr}}$PN$^{\text{Me}}$P)CuBr (**4a**)

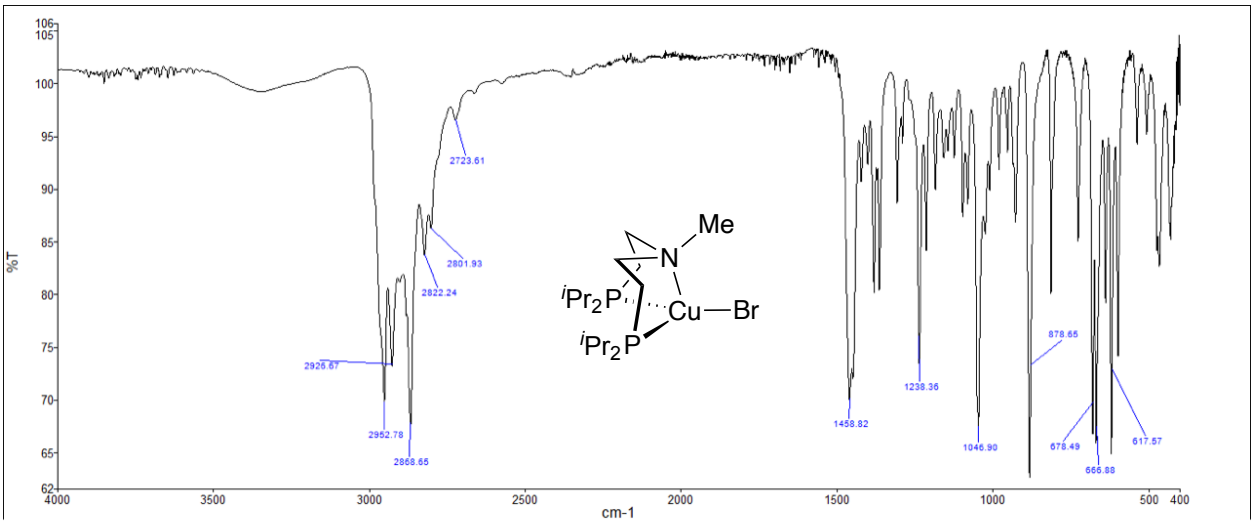

Figure S19. IR spectrum of ($^{i\text{Pr}}$PN$^{\text{Me}}$P)CuBr (**4a**, solid sample)

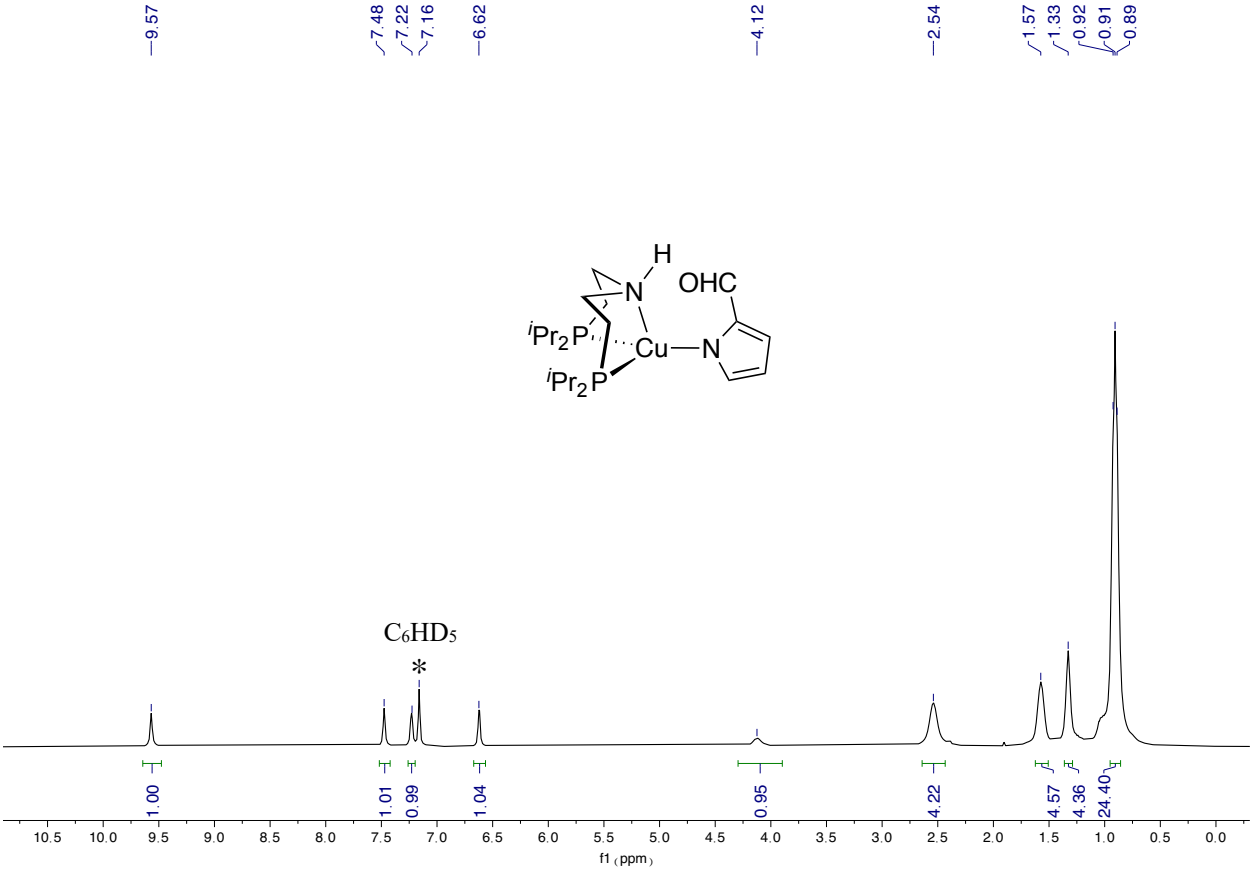

Figure S20. ^{1}H NMR (400 MHz, C_6D_6, 23 °C) spectrum of ($^{i\text{Pr}}$PN$^{\text{H}}$P)Cu(C_4H_3NCHO) (**5a**): 9.57 (s, C*H*O, 1 H), 7.48 (s, pyrrole C*H*, 1H), 7.22 (s, pyrrole C*H*, 1H), 6.62 (s, pyrrole C*H*, 1H), 4.12 (br, N*H*, 1H), 2.66-2.43 (m, 4H), 1.62-1.51 (m, 4H), 1.27-1.29 (m, 4H), 0.95-0.84 (m, CH(CH_3)$_2$, 24H).

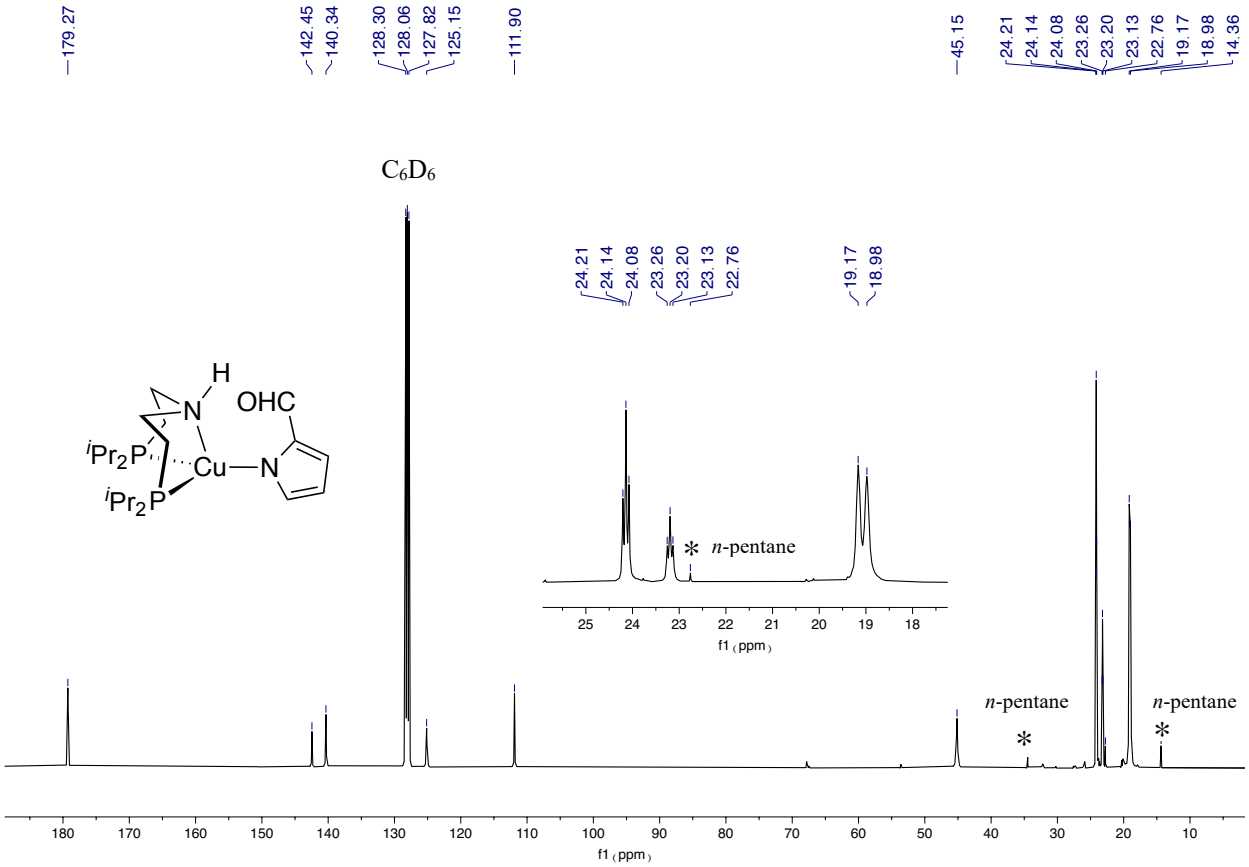

Figure S21. $^{13}C\{^{1}H\}$ NMR (101 MHz, C_6D_6, 23 °C) spectrum of ($^{i\text{Pr}}PN^{H}P$)Cu(C_4H_3NCHO) (**5a**): 179.3 (s, *C*HO), 142.5 (s, pyrrole *C*), 140.3 (s, pyrrole *C*), 125.2 (s, pyrrole *C*), 111.9 (s, pyrrole *C*), 45.2 (s, N*C*H$_2$), 24.2 (t, $J_{C\text{-}P}$ = 6.6 Hz, *C*H(CH$_3$)$_2$), 23.2 (t, $J_{C\text{-}P}$ = 6.3 Hz, P*C*H$_2$), 19.2 (br, CH(*C*H$_3$)$_2$), 19.0 (br, CH(*C*H$_3$)$_2$).

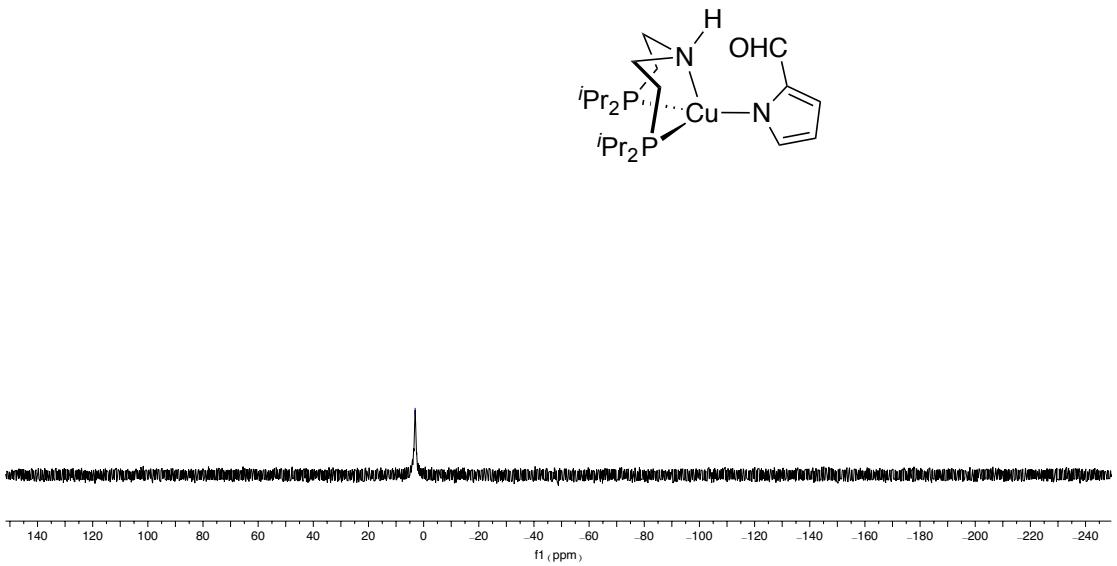

Figure S22. $^{31}P\{^{1}H\}$ NMR (162 MHz, C_6D_6, 23 °C) spectrum of ($^{i\text{Pr}}PN^{H}P$)Cu(C_4H_3NCHO) (**5a**)

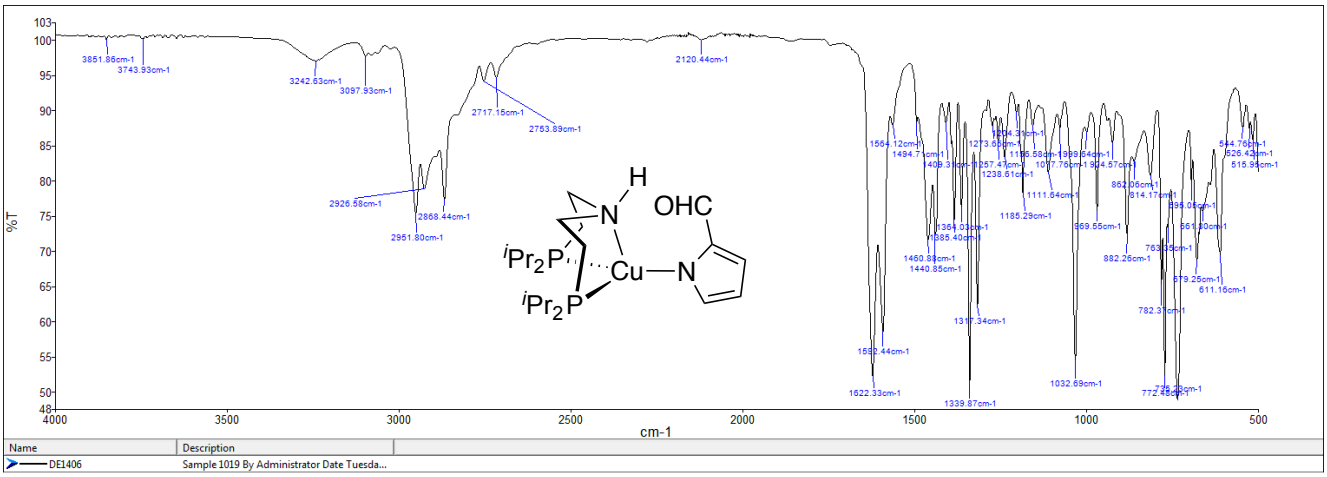

Figure S23. IR spectrum of ($^{i\text{Pr}}PN^{H}P$)Cu(C_4H_3NCHO) (**5a**, solid sample)

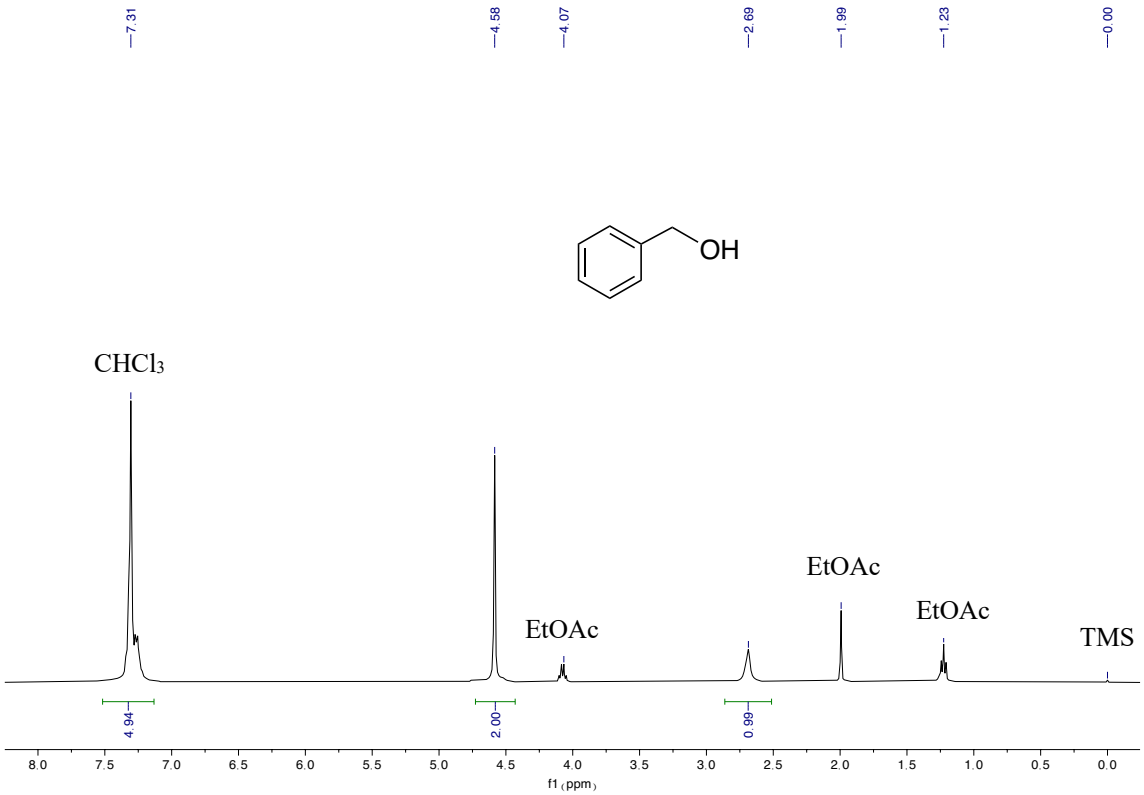

Figure S24. ^{1}H NMR (400 MHz, $CDCl_3$, with TMS, 23 °C) spectrum of benzyl alcohol: 7.53-7.14 (m, Ar*H*, 5H), 4.58 (s, CH_2, 2H), 2.69 (br, O*H*, 1H).

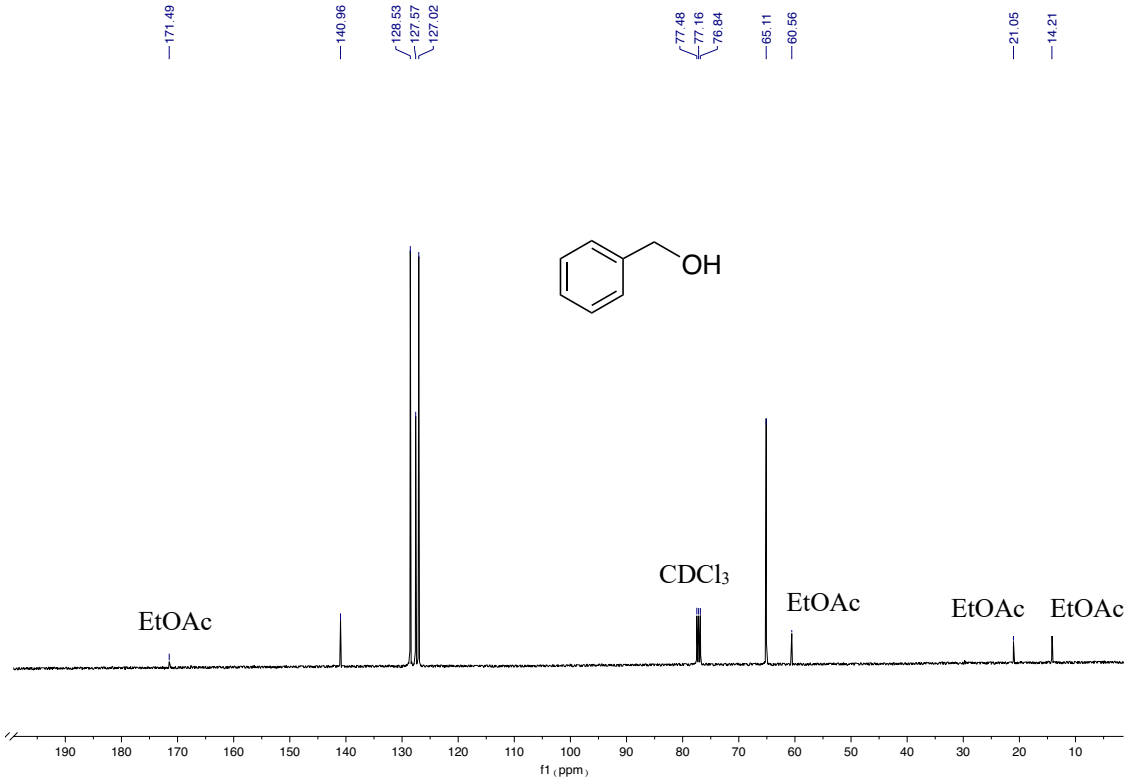

Figure S25. ^{13}C{^{1}H} NMR (101 MHz, $CDCl_3$, with TMS, 23 °C) spectrum of benzyl alcohol: 141.0 (Ar*C*-CH_2), 128.5 (Ar*C*), 127.6 (Ar*C*), 127.0 (Ar*C*), 65.1 (*C*H_2).

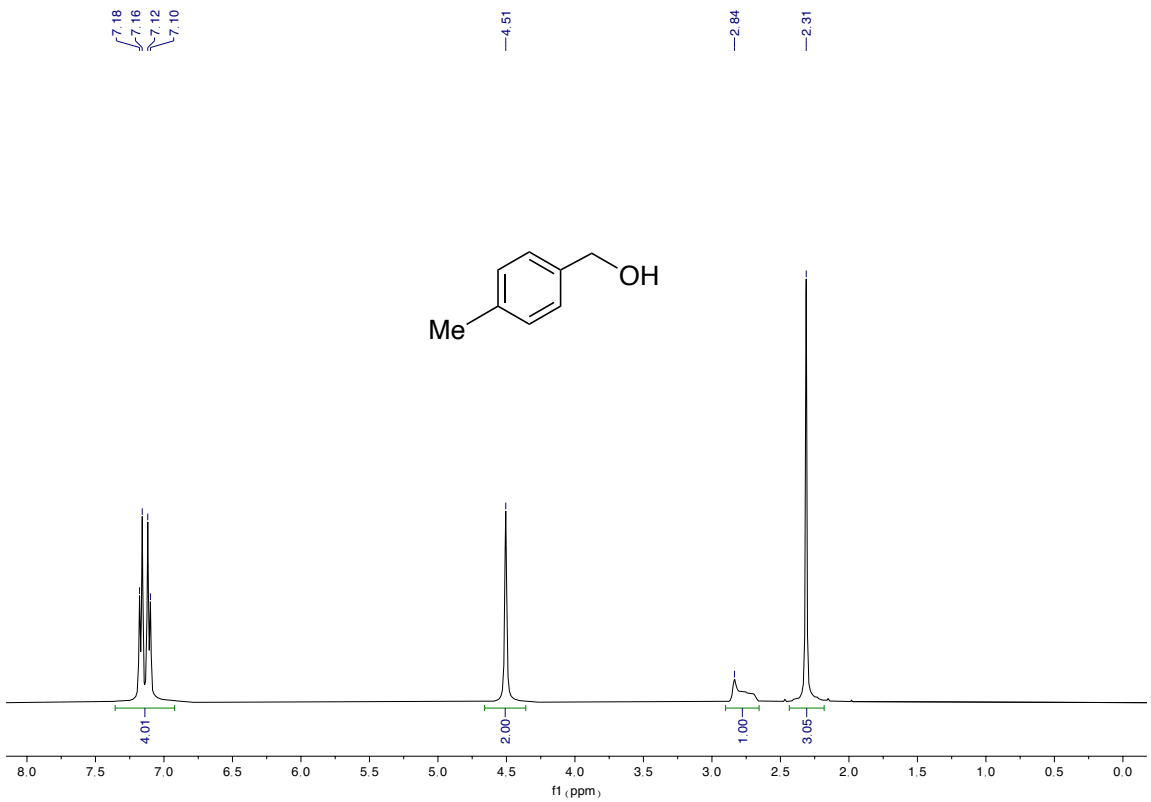

Figure S26. ^{1}H NMR (400 MHz, $CDCl_3$, with TMS, 23 °C) spectrum of 4-methylbenzyl alcohol: 7.36-6.92 (m, Ar*H*, 4H), 4.51 (s, CH_2, 2H), 2.91-2.66 (m, O*H*, 1H), 2.31 (s, CH_3, 3H).

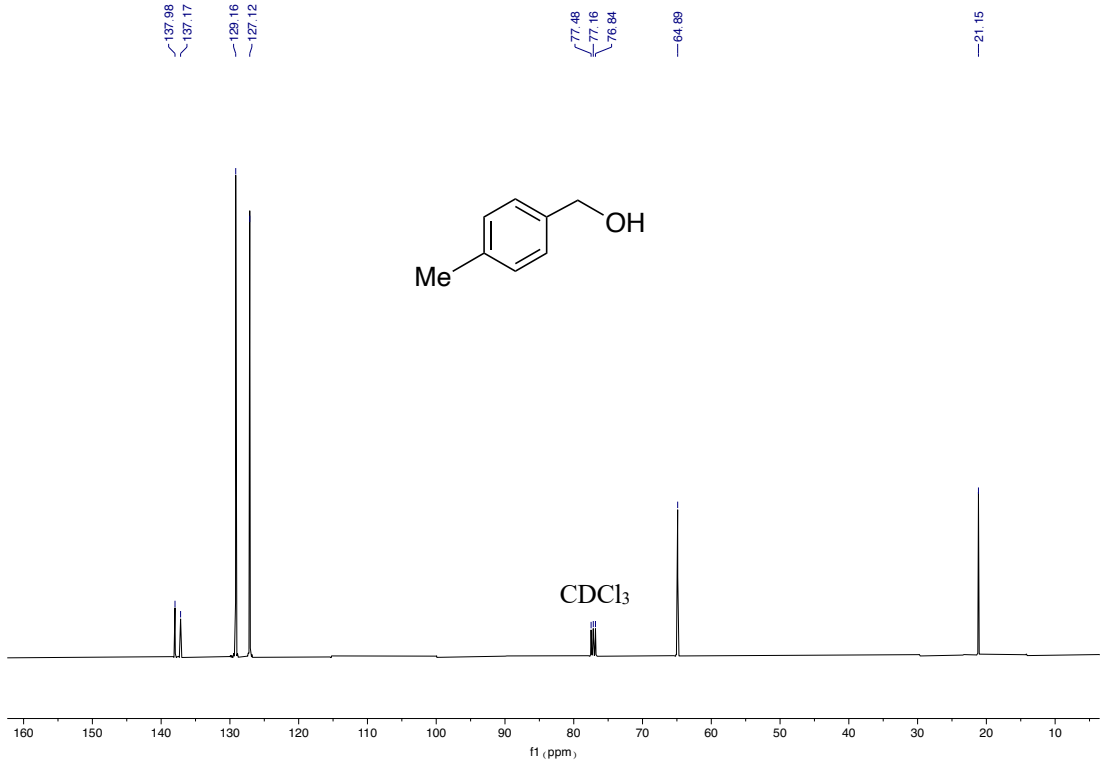

Figure S27. ^{13}C{^{1}H} NMR (101 MHz, $CDCl_3$, with TMS, 23 °C) spectrum of 4-methylbenzyl alcohol: 138.0 (Ar*C*), 137.2 (Ar*C*), 129.2 (Ar*C*), 127.1 (Ar*C*), 64.9 (*C*H_2), 21.2 (*C*H_3).

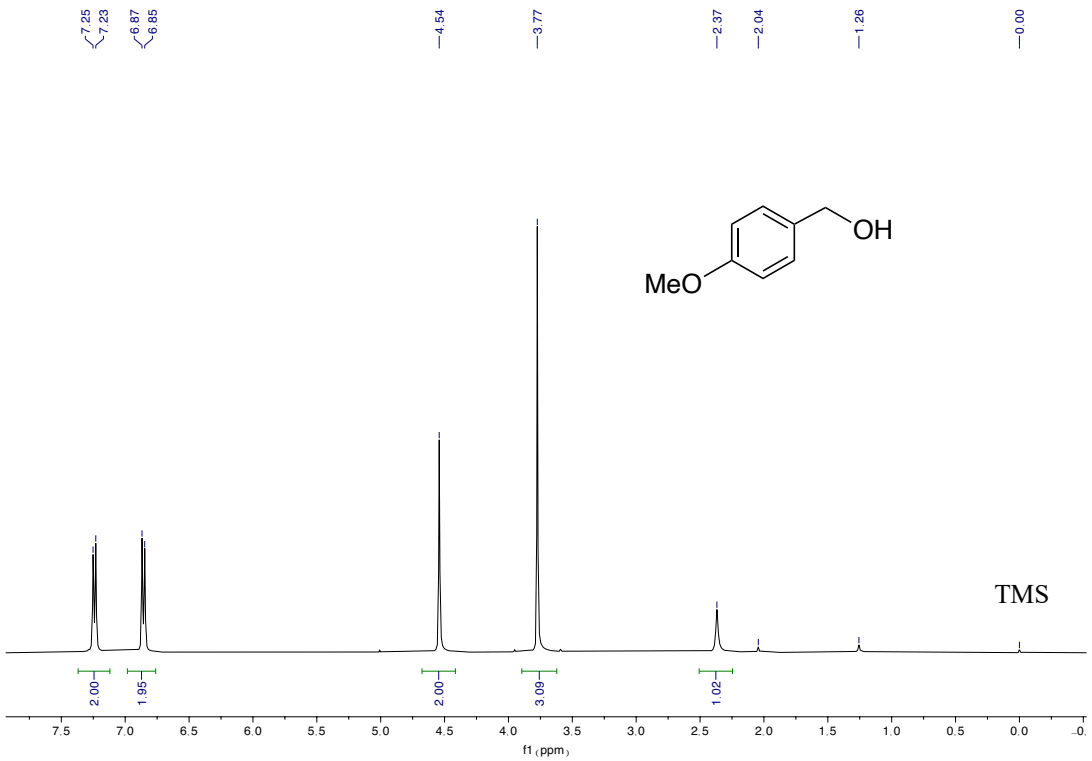

Figure S28. ^{1}H NMR (400 MHz, $CDCl_3$, with TMS, 23 °C) spectrum of 4-methoxybenzyl alcohol: 7.24 (d, $J_{H\text{-}H}$ = 8.6 Hz, Ar*H*, 2H), 6.86 (d, $J_{H\text{-}H}$ = 8.6 Hz, Ar*H*, 2H), 4.54 (s, CH_2, 2H), 3.77 (s, CH_3, 3H), 2.37 (s, O*H*, 1H).

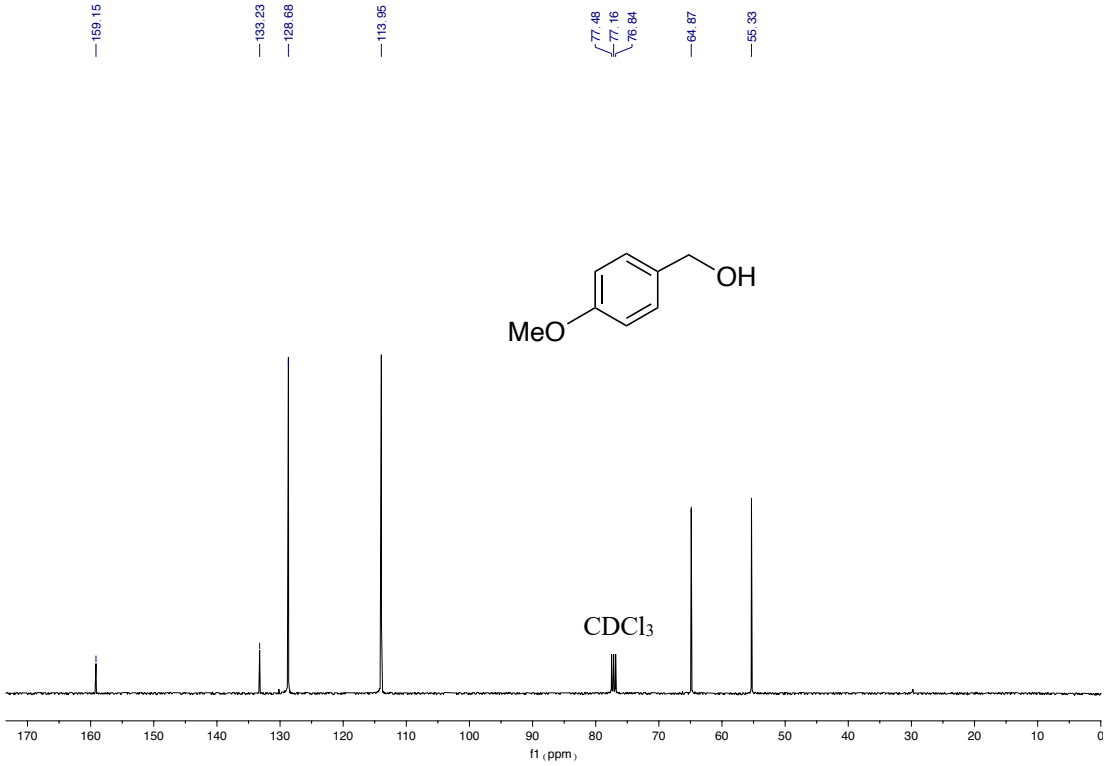

Figure S29. ^{13}C{^{1}H} NMR (101 MHz, $CDCl_3$, with TMS, 23 °C) spectrum of 4-methoxybenzyl alcohol: 159.2 (Ar*C*-OMe), 133.2 (Ar*C*-CH_2), 128.7 (Ar*C*), 114.0 (Ar*C*), 64.9 (*C*H_2), 55.3 (O*C*H_3).

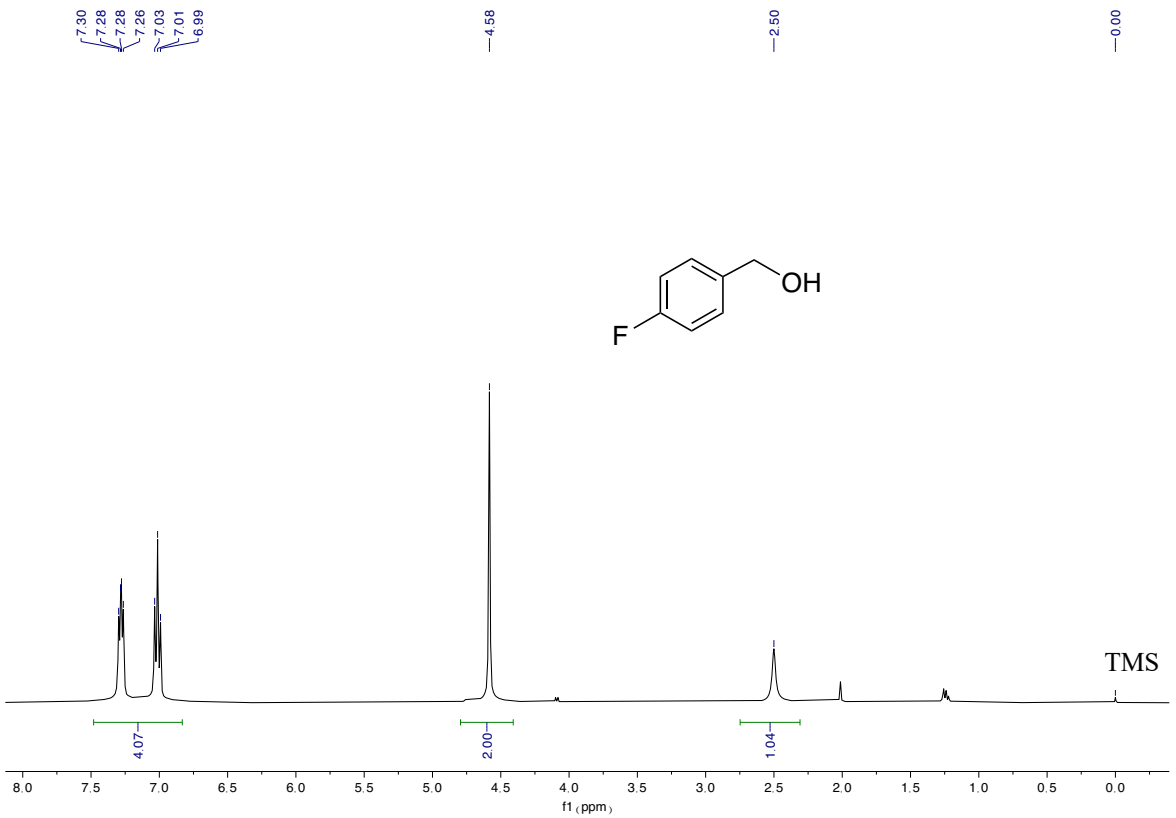

Figure S30. ^{1}H NMR (400 MHz, $CDCl_3$, with TMS, 23 °C) spectrum of 4-fluorobenzyl alcohol: 7.43-7.18 (m, Ar*H*, 2H), 7.13-6.88 (m, Ar*H*, 2H), 4.58 (s, CH_2, 2H), 2.50 (s, O*H*, 1H).

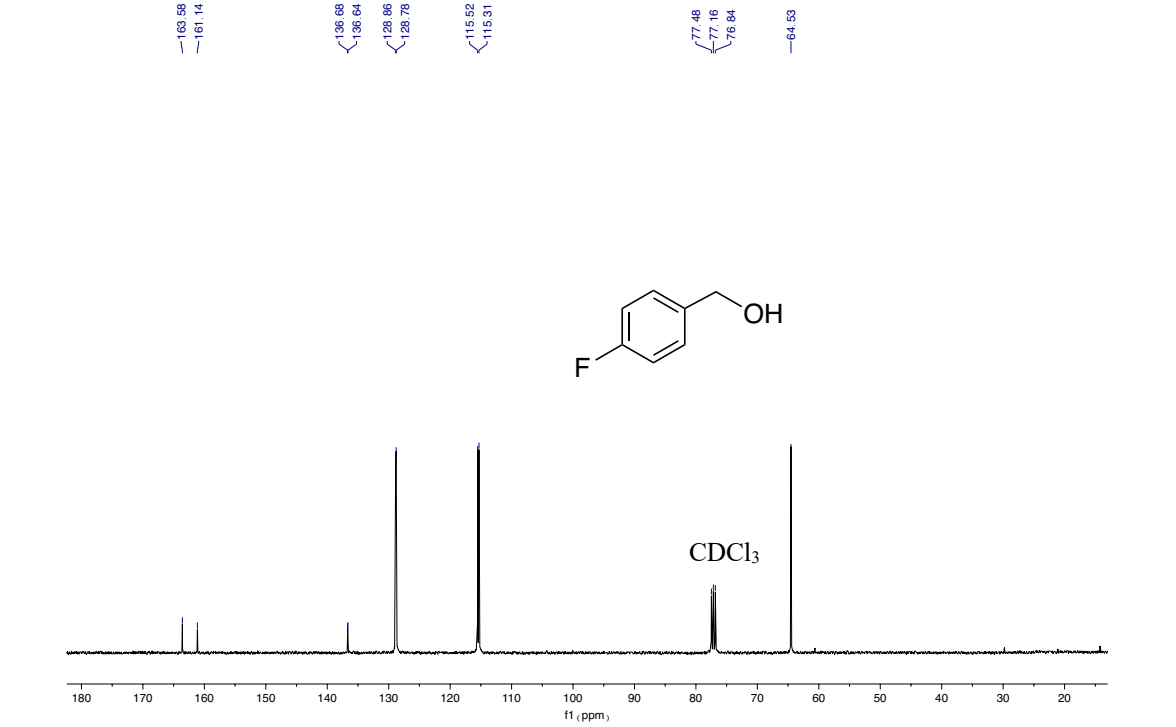

Figure S31. ^{13}C{^{1}H} NMR (101 MHz, $CDCl_3$, with TMS, 23 °C) spectrum of 4-fluorobenzyl alcohol: 162.4 (d, $^{1}J_{H\text{-}F}$ = 246.4 Hz, Ar*C*-F), 136.7 (d, $^{4}J_{H\text{-}F}$ = 4.0 Hz, Ar*C*-CH$_2$), 128.8 (d, $^{3}J_{H\text{-}F}$ = 8.1 Hz, Ar*C*), 115.4 (d, $^{2}J_{H\text{-}F}$ = 21.4 Hz, Ar*C*), 64.5 (s, *C*H$_2$).

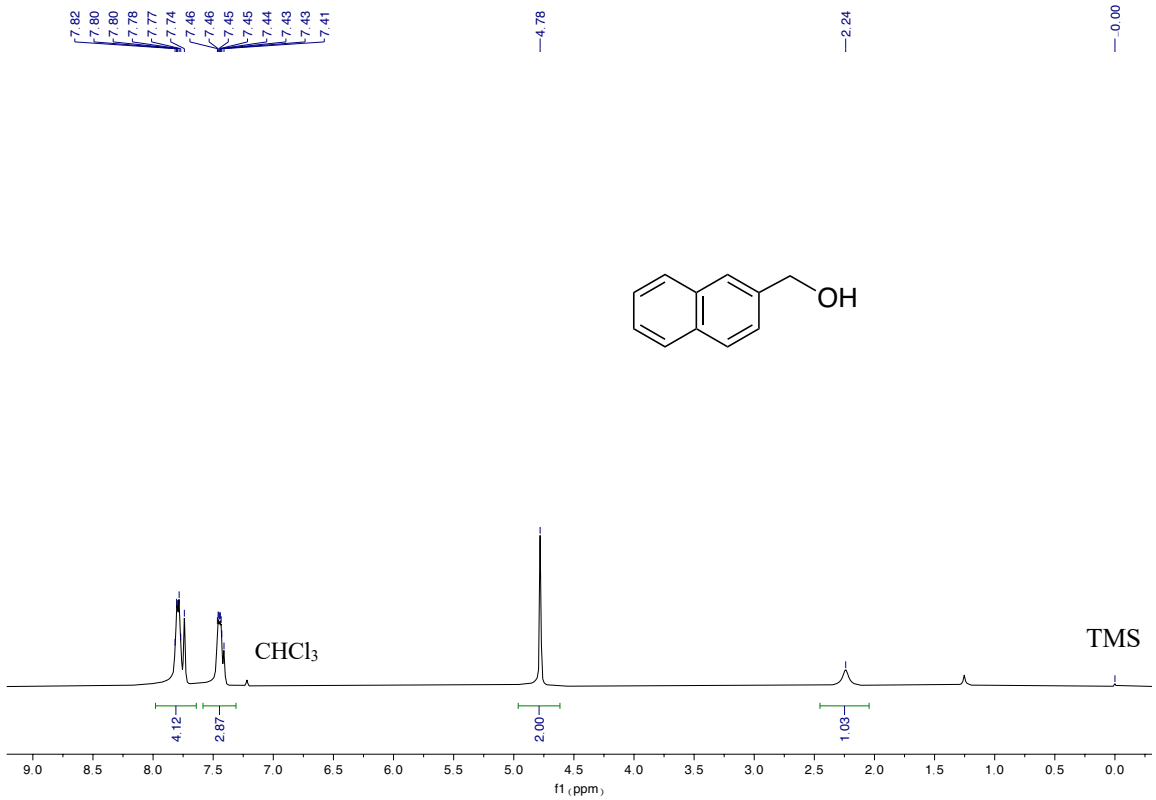

Figure S32. ^{1}H NMR (400 MHz, $CDCl_3$, with TMS, 23 °C) spectrum of 2-naphthalenemethanol: 7.98-7.65 (m, Ar*H*, 4H), 7.58-7.33 (m, Ar*H*, 3H), 4.78 (s, CH_2, 2H), 2.24 (br, O*H*, 1H).

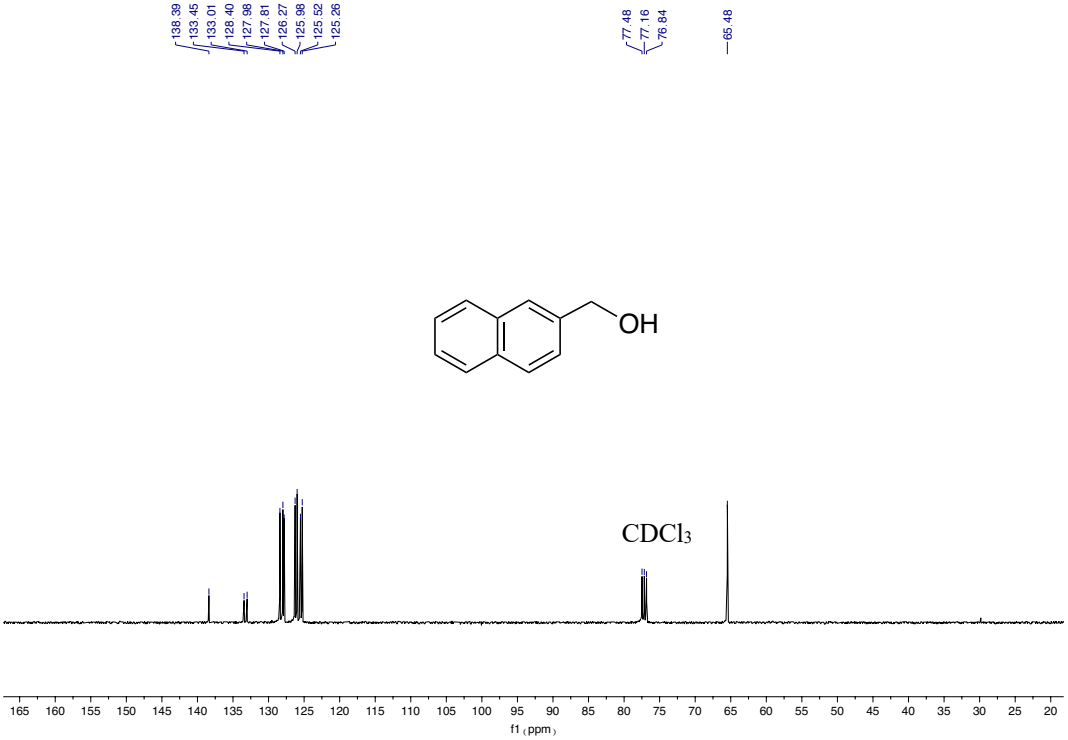

Figure S33. ^{13}C{^{1}H} NMR (101 MHz, $CDCl_3$, with TMS, 23 °C) spectrum of 2-naphthalenemethanol: 138.4 (Ar*C*), 133.5 (Ar*C*), 133.0 (Ar*C*), 128.4 (Ar*C*), 128.0 (Ar*C*), 127.8 (Ar*C*), 126.3 (Ar*C*), 126.0 (Ar*C*), 125.5 (Ar*C*), 125.3 (Ar*C*), 65.5 (*C*H_2).

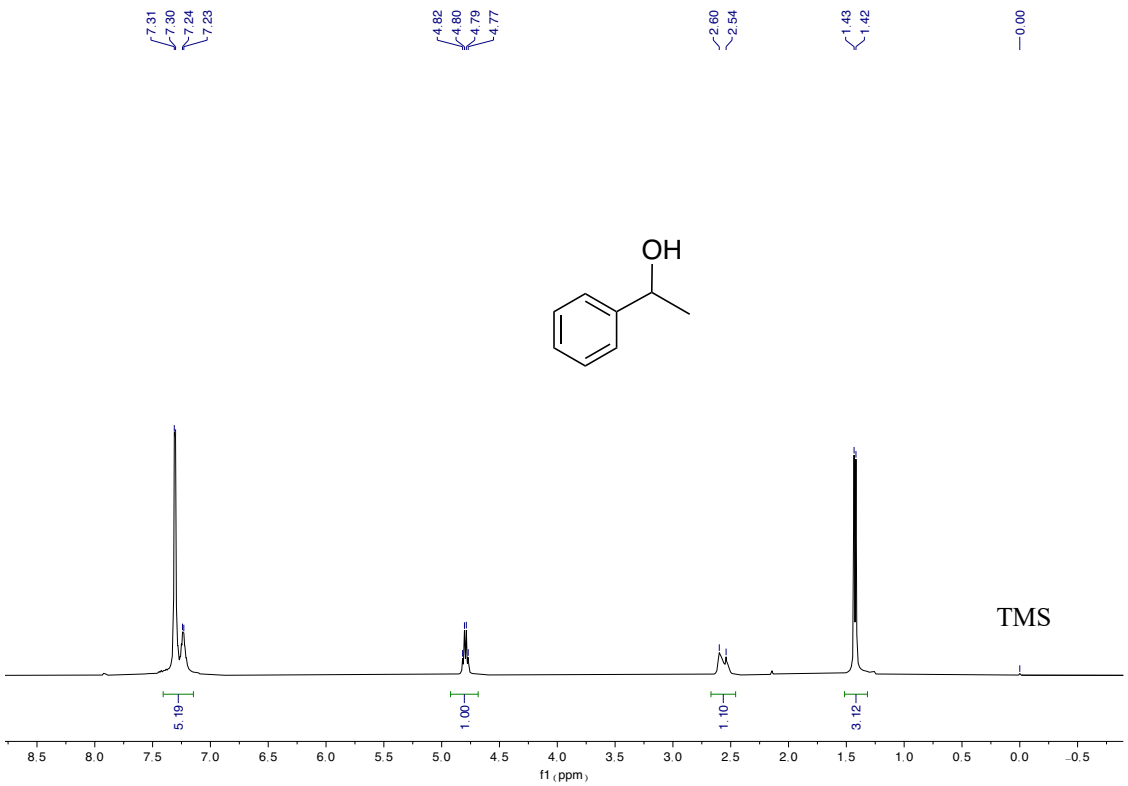

Figure S34. ^{1}H NMR (400 MHz, $CDCl_3$, with TMS, 23 °C) spectrum of 1-phenylethanol: 7.42-7.16 (m, Ar*H*, 5H), 4.80 (q, $J_{H\text{-}H}$ = 6.4 Hz, C*H*OH, 1H), 2.67-2.46 (m, O*H*, 1H), 1.43 (d, $J_{H\text{-}H}$ = 6.4 Hz, CH_3, 3H).

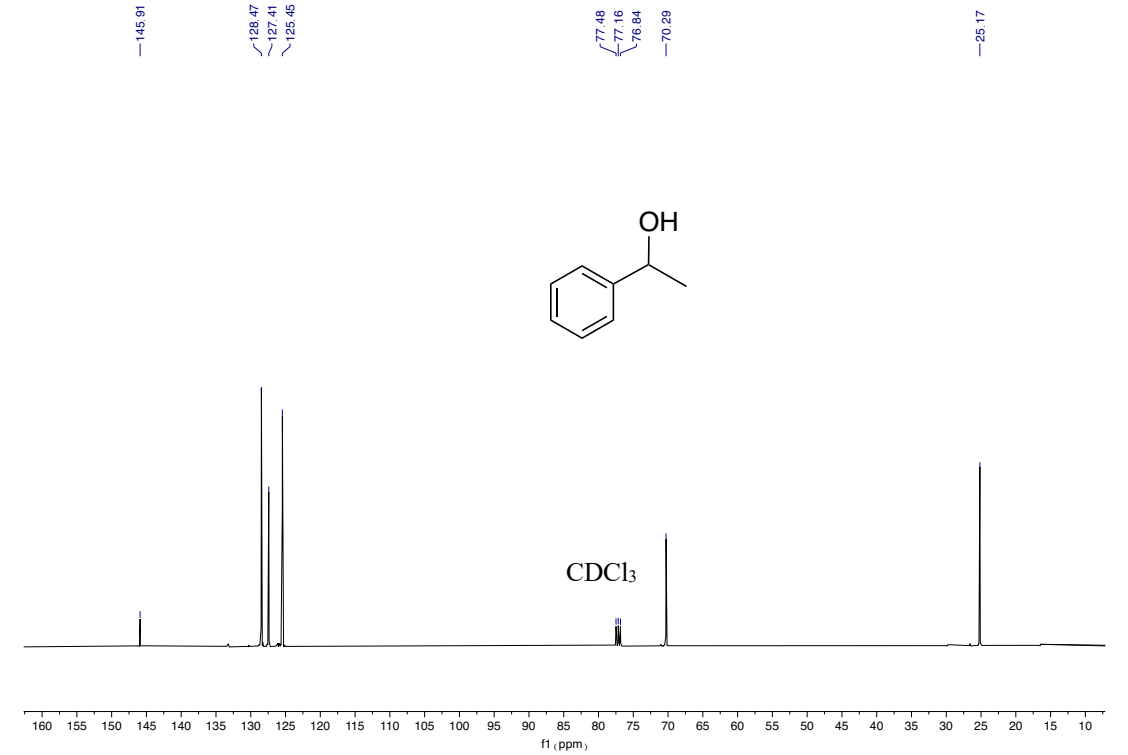

Figure S35. ^{13}C{^{1}H} NMR (101 MHz, $CDCl_3$, with TMS, 23 °C) spectrum of 1-phenylethanol: 145.9 (Ar*C*-CH), 128.5 (Ar*C*), 127.4 (Ar*C*), 125.5 (Ar*C*), 70.3 (*C*HOH), 25.2 (*C*H$_3$).

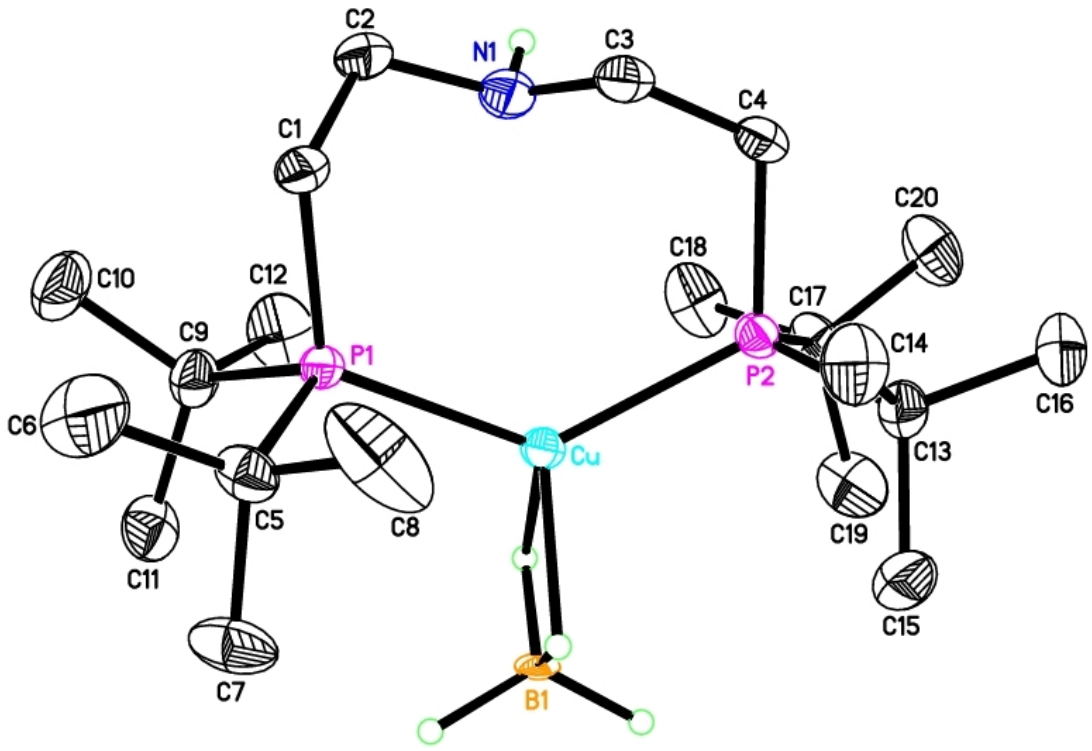

Figure S36. ORTEP drawing of ($^{t\text{Bu}}$PN$^{\text{H}}$P)Cu(BH$_4$) (**2c**) at the 50% probability level (hydrogen atoms bound to nitrogen and boron were located directly from the difference map; the N–H hydrogen coordinate was refined and the B–H hydrogens were held fixed at the located positions during the final stage of refinement; all other hydrogen atoms were calculated and treated with a riding model and omitted for clarity). Selected distances (Å) and angles (deg): Cu–P(1) 2.2784(4), Cu–P(2) 2.2769(4), Cu–B(1) 2.2595(13), Cu…N(1) 3.3397(14); P(1)–Cu–P(2) 130.152(14), B(1)–Cu–P(1) 114.02(4), B(1)–Cu–P(2) 115.82(4), H–Cu–H 65.2.